

Final Report - Section Ozone, Passive Sampling with Summa Canisters and Adsorbent Tubes

Air Quality Monitoring Study to Assess Exposure to Volatile Organic Compounds and Develop Cost-Efficient Monitoring Techniques

Prepared and submitted by:

Detlev Helmig, INSTAAR, Univ. of Colorado
Mike Hannigan, Mechanical Engineering, Univ. of Colorado
Jana Milford, Mechanical Engineering, Univ. of Colorado
Joanna Gordon, Mechanical Engineering, Univ. of Colorado

May 13, 2015

Project Goals as Stated in the Contract are:

1. Develop analytical atmospheric monitoring protocols and refine low-cost, low-maintenance tools for gathering air quality information on oil and natural gas (O&NG) development practices.
 - a. Deploy canister samplers that can capture methane and volatile organic compounds (VOC), which is the traditional VOC monitoring technique, and use these data for evaluating the two new sampling approaches listed below.
 - b. Develop and test low-cost adsorbent tube samplers that can measure VOC, including alkane hydrocarbons and aromatic compounds, with 1 day to 2 week time resolution.
 - c. Deploy and evaluate prototype OG-Pods that can measure a variety of pollutants as described above including ozone, total VOC, and methane.
2. Analyze the air data collected under Goal 1 to further evaluate the fugitive emissions and exposure of residents to ozone, nitrogen oxides (NO_x), and VOC from O&NG operations. Assess exposure gradients in Boulder County to O&NG source pollutants by determining methane and VOC concentrations in air samples from a site on the western boundary of Boulder County and compare those data to four sites near the O&NG operations on the eastern side of the County. Also, compare exposure standards set by the U.S. Environmental Protection Agency for acute and chronic exposure levels.

Accomplished Tasks:

Four air monitoring sites in areas with nearby O&NG production wells in Boulder County were identified. These sites, from north to south were Stephen Day Park in NE Longmont, Dawson School off Highway 285, St Luke's Church in Lafayette, and the Lafayette Fire Station 2. Figure 1 shows a Boulder County map depicting these locations. Monitoring equipment was installed during April – May 2014. Figures 2-5 show site pictures with the installations.

1. The Boulder County Public Health (BCPH) building in the City of Boulder, on the intersection of Broadway and Iris was chosen as 'background' site. This site, while in the heart of the City of Boulder, is on the western edge of the Colorado Front Range and ~15 miles away from the East Boulder County line from which O&NG operations extend towards the east to northeast. A photograph showing the installation at this site is given in Figure 6.
 2. Five traditional passive canister combined with new absorbent tube sampling packages for time-integrated air collection were assembled.
 - a. Whole air samples collected in canisters at constant flow rate using commercial constant flow sampling devices (Figure 7). These air samples were subsequently subjected to analysis of methane and VOC in the C2-C7 carbon range, including the aromatic compounds benzene, toluene, ethylbenzene, and xylenes (= BTEX) at INSTAAR.
 - b. Air was also collected by diffusion (passive sampling) onto tubes that are packed with carbon-based adsorbents (Figure 7). These tubes are pre-conditioned in the lab, sealed, and then taken to the site. For sampling, one side of the cartridge is opened so that VOC can diffuse into the tubes and be retained on the adsorbents. At the sites adsorbent tubes were housed inside a canister, with an open bottom side (similar to an upside-down coffee can), to prevent exposure to dust and moisture. At the end of the sampling tubes are collected, sealed, and taken to the laboratory at INSTAAR for thermal desorption and chemical analysis.
 - c. Temperatures for the canisters and cartridges during the collection periods were monitored with small USB stick temperature and humidity data loggers.
 3. Five OG-Pods were equipped with wind speed*, wind direction*, temperature, relative humidity, ozone, nitrogen oxide (NO), nitrogen dioxide (NO₂), carbon monoxide (CO), carbon dioxide (CO₂), total VOC, and methane sensors. (* Indicates only three of the sites: St. Luke Church, BC Public Health, and Stephen Day Park.). The sensor for hydrogen sulfide (H₂S) mentioned in the proposal as a possibility for the study was not available to be deployed.
 4. These three types of equipment (canister, adsorbent tube, OG-Pod) were deployed at these five sites from mid-May through late August. Canisters and cartridges were deployed for 3-5 days during a total of 14 periods. OG-pods were deployed from May 7th – August 28th. They were on site continuously through this time, interrupted only by a week for calibration in June and July as well as several short periods dedicated to maintenance and repair. In addition, a UV absorption ozone monitor was operated continuously at Dawson School. The sampling schedule is shown in Figure 8.
 5. On 11 occasions adsorbent cartridges were deployed in pairs to investigate the reproducibility of the measurement. Canister and cartridge samples were analyzed in the trace gas laboratory at INSTAAR on a gas chromatography system. In total, data from 62 canister and 71 adsorbent tube samples were obtained.
 6. The deployment of the OG pods yielded a total of ~2000 hours of observations at each site.
 7. Four approximately week-long co-location calibrations took place among all five OG-Pods and reference instruments at CAMP in Denver (a Colorado Department of Public Health and Environment operated air quality monitoring station). These co-locations are used to generate calibration functions for ozone, NO, NO₂, CO₂, and CO to quantify sensor signals.
 8. Calibration functions were developed for the OG-Pod sensors for the following species: ozone, NO, NO₂, CO₂, and CO.
 9. An exploratory co-location with a Picarro cavity ring-down methane analyzer was conducted to investigate calibration functions for the OG-Pod methane sensors.
-

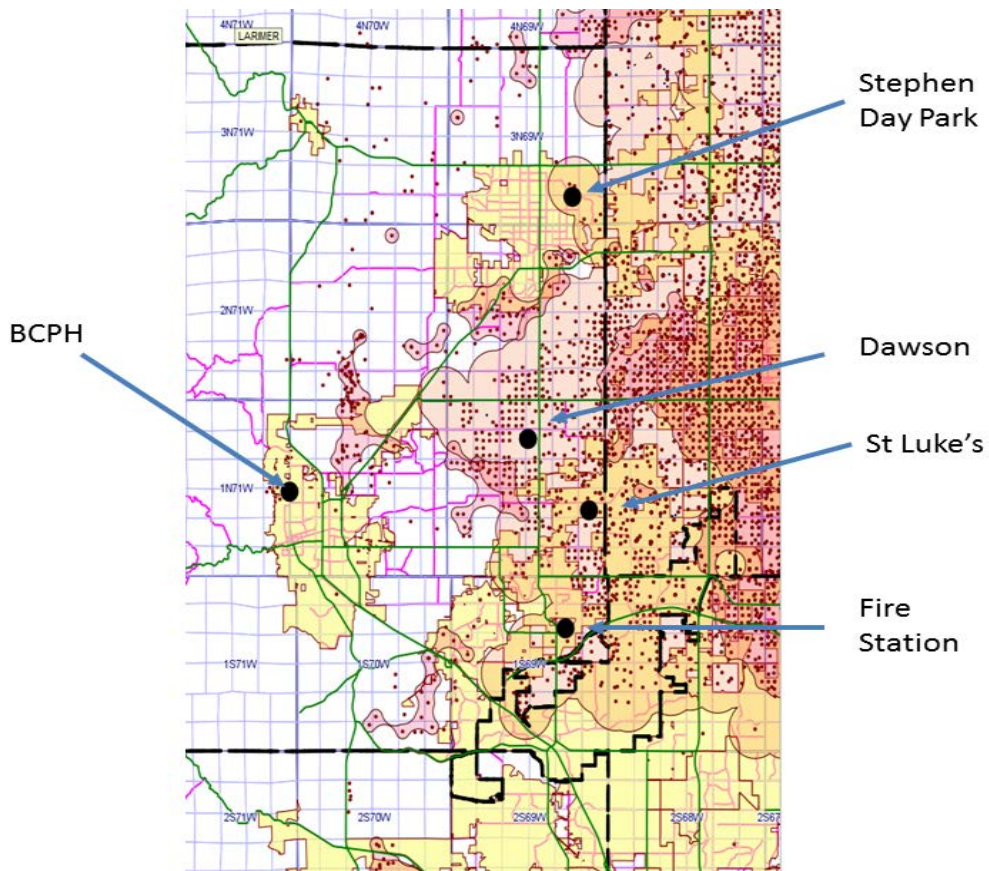


Figure 1
 Location of five sampling sites indicated by black dots, the Boulder County Public Health Department, Stephen Day Park, Dawson Elementary School, St Luke's Church, and Lafayette Fire Station. Smaller size red dots show locations of O&NG wells, derived from GIS data obtained from the COGCC website. The dashed black line shows the Boulder County border.



Figure 2
Sampling equipment on the roof of a shelter in Stephen Day Park in Longmont.



Figure 3
Samplers installed on the roof of a maintenance building on the grounds of Dawson School. The OG-POD is in the red box on the mast, the cylindrical housing for the adsorbent tube is at the right, and a cooler containing the summa canister is secured to the platform.



Figure 4
Sampling setup at St. Luke's church in Lafayette.

Figure 5
Sampling arrangement on the roof of Lafayette Fire Station Number 2.

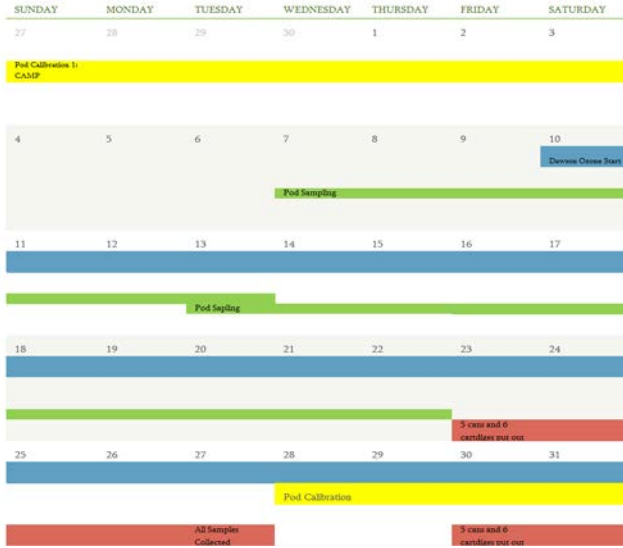


Figure 6.
Sampling setup on the roof of the BCPH building.



Figure 7.
Stainless steel Summa canister with passive sampling flow regulator (right) and two solid adsorbent cartridges for VOC sampling (front left) shown side by side.

May 2014



July 2014



June 2014



August 2014



Legend

- Pod Calibration
- Dawson Ozone Monitor
- Pod Sampling
- Can and Cartridge Sampling

Figure 8.

Deployment schedule showing the operation of ozone monitor, canisters, adsorbent cartridges, and OG-Pods at the five sampling sites. All sampling was done concurrently at all locations, except for the ozone monitoring with the commercial instrument, which was operated at Dawson School only. The last OG-Pod calibration was continued until Sept. 6, and ozone monitoring at Dawson was continued through October 28.

Results

Evaluation of passive sampling on adsorbent cartridges for monitoring of oil and natural gas emissions

The suitability of adsorbent cartridges for passive sampling of oil and natural gas VOC was evaluated using several approaches, discussed in the following.

Parallel sampling of whole air canister samplers and cartridges at field sites. Canisters and cartridges were deployed side-by-side at each of the sampling sites as shown in Figure 3. Air was pulled at constant flow by the vacuum in the canisters. The flow apparatus used was specified to attain 60-hours constant rate sampling. However, we observed a loss of flow rate into the canisters after 3-4 days from the canister filling up a bit quicker than specified, and from not being exposed to the full pressure differential that would be observed at sea level. Consequently, we reduced the sampling interval to ~3 days three weeks into the experiment, which then more consistently provided constant sampling rates throughout the deployment period. Adsorbent cartridges were sampled during these same time intervals, yielding ~3 days of integrated sampling. Results from these side-by-side sampling are shown in Figure 9 for the primary VOC classes that are of interest. Correlations of normalized collection rates of analyzed VOC between adsorbent cartridges and canisters showed high variability between compounds, with some species showing very good (tight correlations), i.e. propane, butanes, pentanes, and other compounds (ethane, alkenes) showing poorer correlations. For compounds exhibiting strong correlations the cartridge technique appears to be a viable and very simple method for monitoring these compounds in ambient air. In particular, and luckily for our project goals, the adsorbent method appears to work very well for primary O&NG emissions indicator compounds, such as propane, *iso*-butane, and *n*-butane (these are all non-methane hydrocarbons (NMHC)). The adsorbent seems to be too weak to capture the most volatile NMHC ethane.

Paired parallel sampling of whole air canister samplers and cartridges at INSTAAR. This experiment was repeated in November/December by parallel sampling of canisters and adsorbent cartridges over three weeks outside of INSTAAR (30th/Marine). During this experiment all samples were collected in pairs to investigate and compare the reproducibility of both methods. Results shown in Figure 10 show similar relationships and are in good agreement with the summer study, with good correlations for the light alkane compounds (propane – hexane), and poorer correlations for ethane and the alkenes. Results for aromatic VOC were in between, yielding R² correlation coefficients between 0.4-0.7. Results show that both methods display variable repeatability, with both methods working well for alkane VOC, with relative standard deviations <10% for the C3-C6 alkanes. Given that the repeatability is generally better than the correlation between both methods it appears that there are some variables that exert different influence on the sampling, respectively passive uptake rates for both methods. One possible candidate variable is the temperature encountered during sampling. For each sampling interval temperature recorded with the USB temperature data loggers were retrieved and relationships between the cartridge/canister results as a function of temperature were investigated. We did not see any obvious dependency in these data. Consequently, there likely must be other influences that influence the agreement between both methods, such as winds during the sampling interval. Unfortunately, wind data were not recorded, so this possible influence cannot be further investigated at this time.

Investigation of linearity of VOC uptake by sampling of standard air. An important requirement for the passive sampling method to be a feasible field method is that uptake of VOC over time occurs at a constant rate and that sampling is conducted before the adsorbents become saturated. In order to investigate this dependency a set of cartridges was placed in a Tedlar bag which was purged

continuously with a VOC standard. One pair of cartridges was removed every day over a period of ten days. This experiment was conducted two times with similar results. Results from the second experiment are shown in Figure 11. Findings were similar in that good results, i.e. linear uptake was seen for the light alkane (except ethane) VOC. Alkenes were less reproducible and results for aromatic compounds were somewhere in between. These results show that for the primary oil and natural gas emissions, i.e. light alkanes, the cartridge method yields good linear uptake behavior which allows integrated sampling of these gases over extended periods, spanning to at least two weeks.

Conclusions of the VOC Analytical Method Testing

Experiments conducted in the context of this study showed that the selected methods, materials, and methodology yielded good quality results that demonstrate the suitability for O&NG emission monitoring. Sampling of whole air into stainless steel canisters is a well-established method. In this study, we deployed passive sampling kits that facilitated the gradual sampling of air into the canisters, allowing collection of air and obtaining data that represent average concentration levels that were encountered during the sampling interval. Under the atmospheric pressure conditions that are present in the Colorado Front Range these samplers performed well and reliably for at least three days. After that individual units started deviating somewhat. We therefore recommend not extending sampling intervals for longer than three days. In this study adsorbent tubes were housed inside a canister, with an open bottom side (similar to an upside-down coffee can), mostly to prevent contamination from dust and moisture and heating from direct sun light exposure. The same adsorbent tubes can also be carried on people, to monitor personal exposure. As a matter of fact, a special clip is available that allow attaching tubes a shirt pockets like a ball pen; this monitoring approach has previously been used extensively in work place exposure assessments. The data comparisons of the parallel sampling of adsorbent cartridges with the canisters showed mixed results for individual VOC species. Findings were consistent within a series of experiments that were conducted, including the summer sampling at the field sites, a second similar study in late fall at INSTAAR, and two laboratory experiments that investigated the uptake rates over time. For ethane and unsaturated VOC, correlations were weak. Under the so far applied analytical conditions monitoring of these species does not seem feasible. For the light n-alkane VOC, in particular propane, and isomers of butane, pentane, and hexane, the passive sampling yielded good results, demonstrating that the cartridge method is applicable to the monitoring of these species. Furthermore, results for aromatic VOC, in particular BTEX were promising. Correlations were not quite as strong, but we feel that they are good enough to facilitate monitoring for a first assessment of exposure levels for these compounds. Analytical work is currently continuing to further improve the method performance for the aromatics. Light n-alkane VOC have been identified at the primary O&NG emissions. Therefore, we consider the passive monitoring using adsorbent cartridges a suitable method for monitoring exposure to O&NG emissions. This method has numerous advantages over traditional VOC measurement techniques. These include:

- It provides a time-integrated, average exposure assessment.
- Data for individual VOC species are obtained.
- Sensitivity to below ppb levels can be achieved, which is well suitable to identify conditions of elevated exposure.
- Samplers are small and can be deployed in pretty much any type of sampling environment.
- Very little training/instructions are needed for proper deployment of samplers.
- Sampling cartridges are low cost, on the order of ~\$100 and can be re-used many times.
- Many cartridges can be deployed in parallel, allowing for surveys of spatial gradients in exposure.

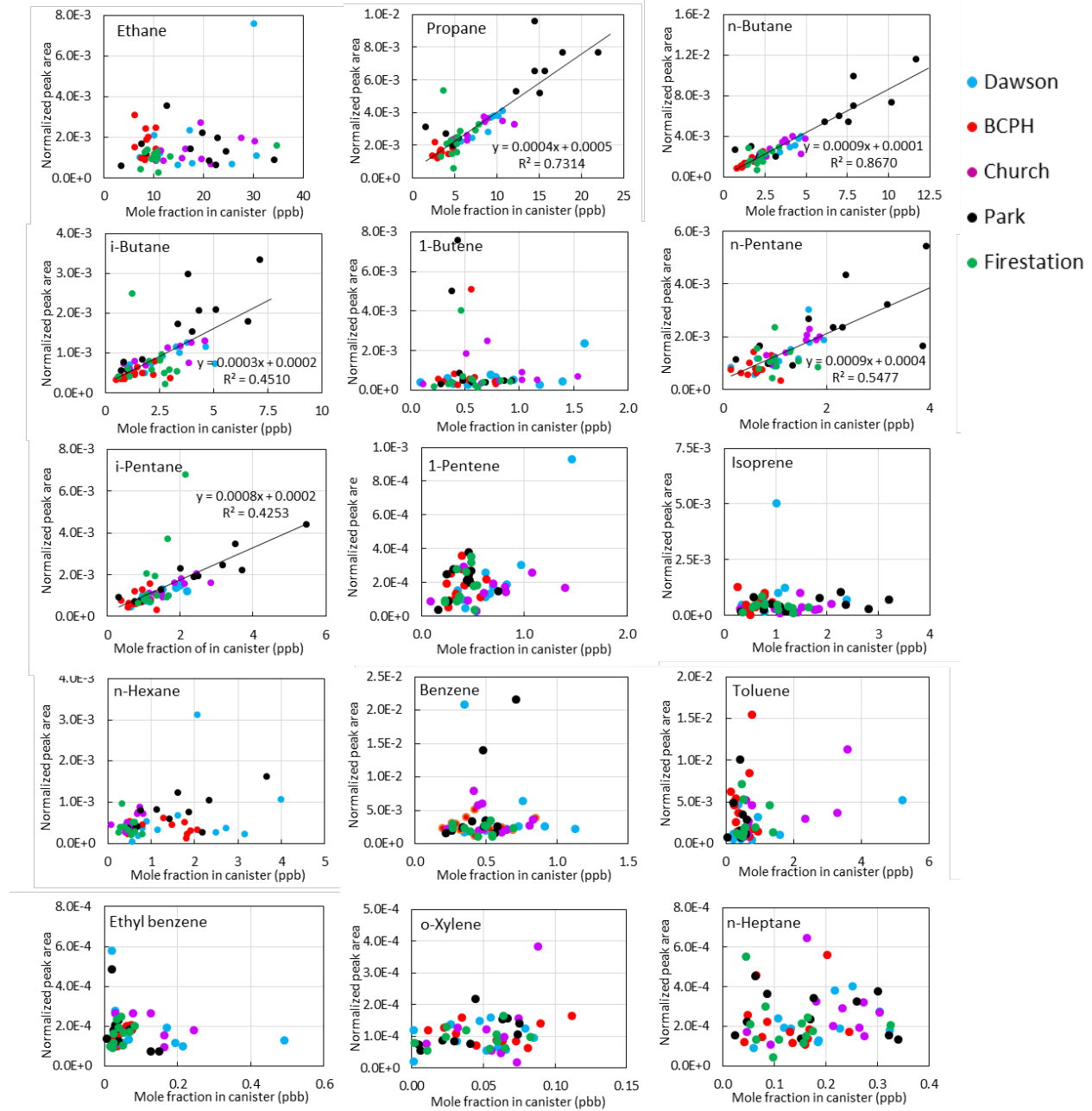


Figure 9

Comparison of results from the quantification of VOC in canisters (reference method, x-axis) with results from the passive sampling of adsorbent cartridges (Y-axis). The cartridge data were normalized to the length of the sampling period and the carbon number of the respective molecule. Results are grouped by sampling sites according to the legend. Results for linear regression correlation analyses are given in cases where correlations gave $R^2 > 0.4$.

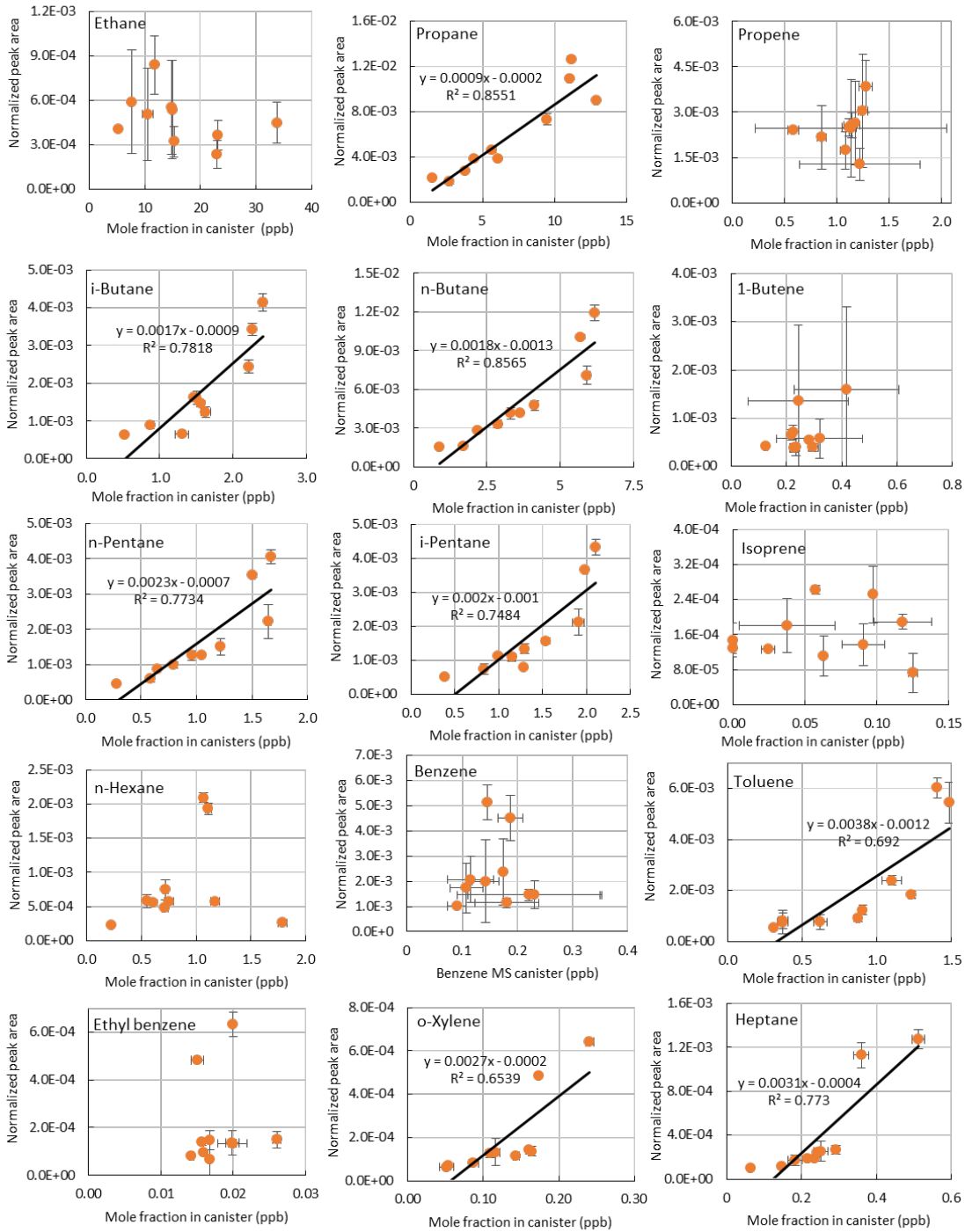


Figure 10

Comparison of results from the quantification of VOCs in canisters (reference method, x-axis) with results from the passive sampling of adsorbent cartridges (Y-axis) for samples collected in outside air at INSTARR on Marine/30th Street during Nov – Dec. 2014. The cartridge data were normalized to the length of the sampling period and the carbon number of the respective molecule. Each sample collection was done in pairs. Error bars indicate the 1-σ standard deviation of the paired results. Results for linear regression correlation analyses are given in cases where correlations gave $R^2 > 0.4$.

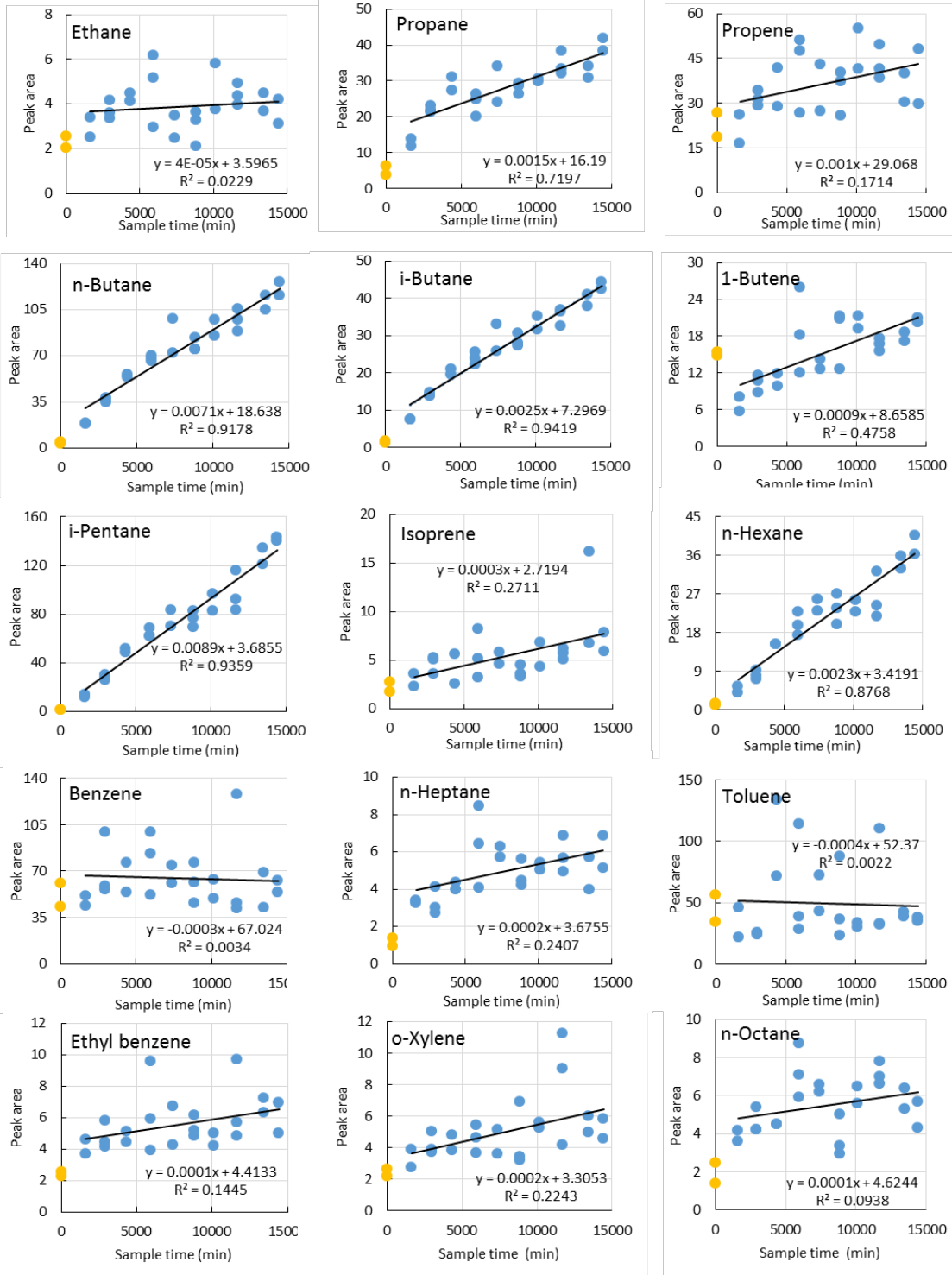


Figure 11

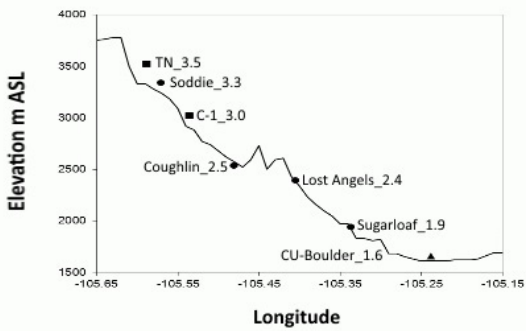
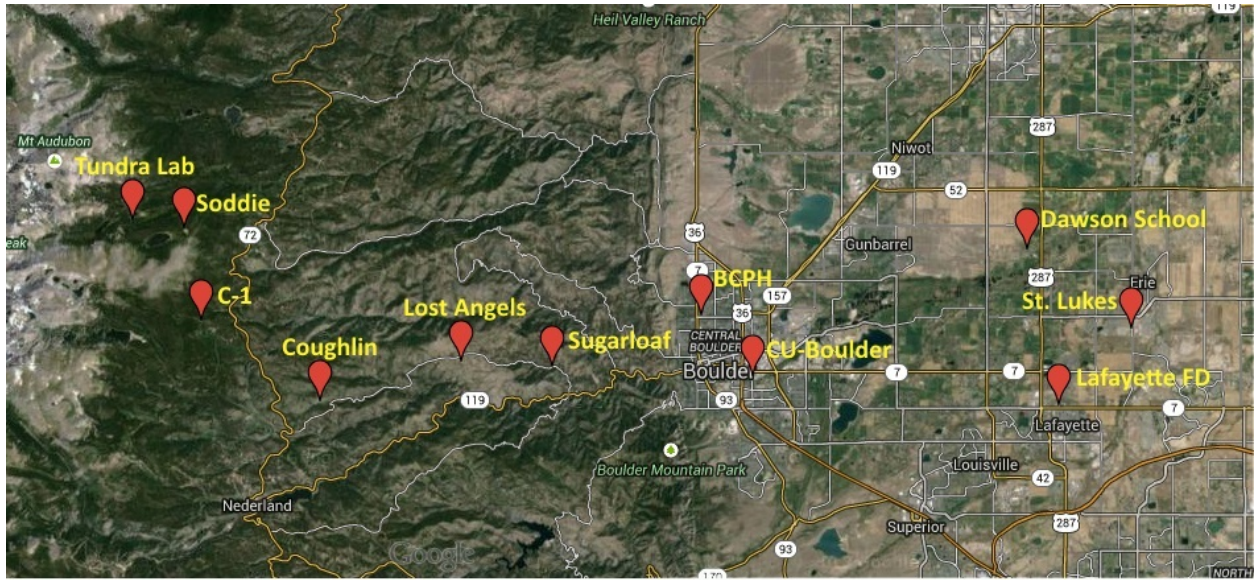
Uptake VOCs onto adsorbent cartridges in a laboratory experiment where cartridges were placed inside a Tedlar bag that was purged with a gas mixture from a compressed air cylinder. The experiment was continued over ten days with pairs of cartridges removed every day and then analyzed by GC-FID. Blank values are included as yellow points.

- Cartridges can be prepared and distributed on very short time scales (~1 day).
- Analysis of collected cartridges can be done at INSTAAR at comparatively low cost.

Ozone measured by a commercial UV absorption monitor at Dawson

INSTAAR operated four other monitoring sites in the context of the Front Range Air Pollution and Photochemistry Experiment (FRAPPE). In Figure 12, the distribution of these sites, in addition to two sites operated by NOAA within Boulder County is shown. The ozone record collected at Dawson is shown individually and compared with data from these other sites in Figure 13a. These comparisons show that there are common features in the ozone distribution within Boulder County, indicating that regional ozone production is a determining process. There are, however, local features that are particular for each site. Ozone at Dawson on many days was the or close to the highest levels seen in the County. However, there are also several days where ozone at Dawson is lower than levels seen at other sites. Ozone is generally higher in the outskirts of the city of Boulder. Similar findings were presented in a previous study from a chain of monitoring stations stretching from Boulder to the Continental Divide at Niwot Ridge (Brodin et al., 2010). This study showed highest mean ozone levels at elevations ~500-1000 m above the plains along the mountain slopes. Similarly, the five-site comparison among lower elevations sites in Boulder County during the 2007-2008 Air Toxics Study ((Eisele et al., 2008) showed lowest ozone levels right within the City of Boulder. These gradients are mostly driven by lower lighttime ozone within the City from titration of ozone with nitrogen oxide emitted by local sources. .

Ozone was highly variable, as typical for this region, with ozone maxima typically occurring in the afternoon due to daytime photochemical production. The maximum 1-hour ozone of 90.9 ppb was observed on July 3. The maximum 8-hour mean of 75 ppb was observed on July 22. The current US National Ambient Air Quality Standard (NAAQS) for surface ozone is defined as 75 ppbv for the 8-hour average, the U.S. Environmental Protection Agency (EPA) has proposed lowering this standard to between 60-70 ppbv in the near future. For comparison, in the European Union the standard is 62 ppbv and in Canada it is 60 ppbv. During the 2015 summer 1-hour ozone ≥ 75 ppbv was observed on 37 hours on 15 days, and 8-hour average ozone ≥ 75 ppbv was observed on 1 day (July 22). Figure 14 compares the 4th highest 8-hour ozone reading from five sites during 1999-2014. This record shows that the 2014 summer was a relatively low ozone year, compared to previous years, which likely was driven by relatively cooler and less sunny weather conditions that were prominent last year.



Site Name	Location	Elevation
Tundra Lab	40° 3' 17" N, 105° 35' 21" W	3528 m
Soddie	40° 2' 52" N, 105° 34' 15" W	3345 m
C-1	40° 2' 9" N, 105° 32' 9" W	3021 m
Coughlin	40° 0' 13.27" N, 105° 28' 43.31" W	2523 m
Lost Angels	40° 1' 8.45" N, 105° 24' 17.96" W	2392 m
Sugarloaf	40° 1' 1.22" N, 105° 21' 27.39" W	1978 m
CU-Boulder	40° 0' 48.2" N, 105° 15' 10.9" W	1607 m
Lafayette FD	40° 0' 6.4" N, 105° 5' 38.8" W	1600 m
BCPH	40° 2' 13.97" N, 105° 16' 52.9" W	1569 m
Dawson	40° 3' 50.2" N, 105° 6' 36.8" W	1562 m
St. Lukes	40° 1' 56" N, 105° 3' 24.2" W	1550 m

Figure 12

Top: Map of Boulder County Front Range area showing seven sites on an east-west transect where ozone was measured within the FRAPPE study. Bottom: Graphical representation of the elevation cross-section. Abbreviations used stand for Tundra Lab, Soddie, C1 (Mountain Research Station), Coughlin, Los Angels, Sugarloaf, and CU Boulder. Also included for reference are four of the sites that were included within the framework of the Boulder County study.

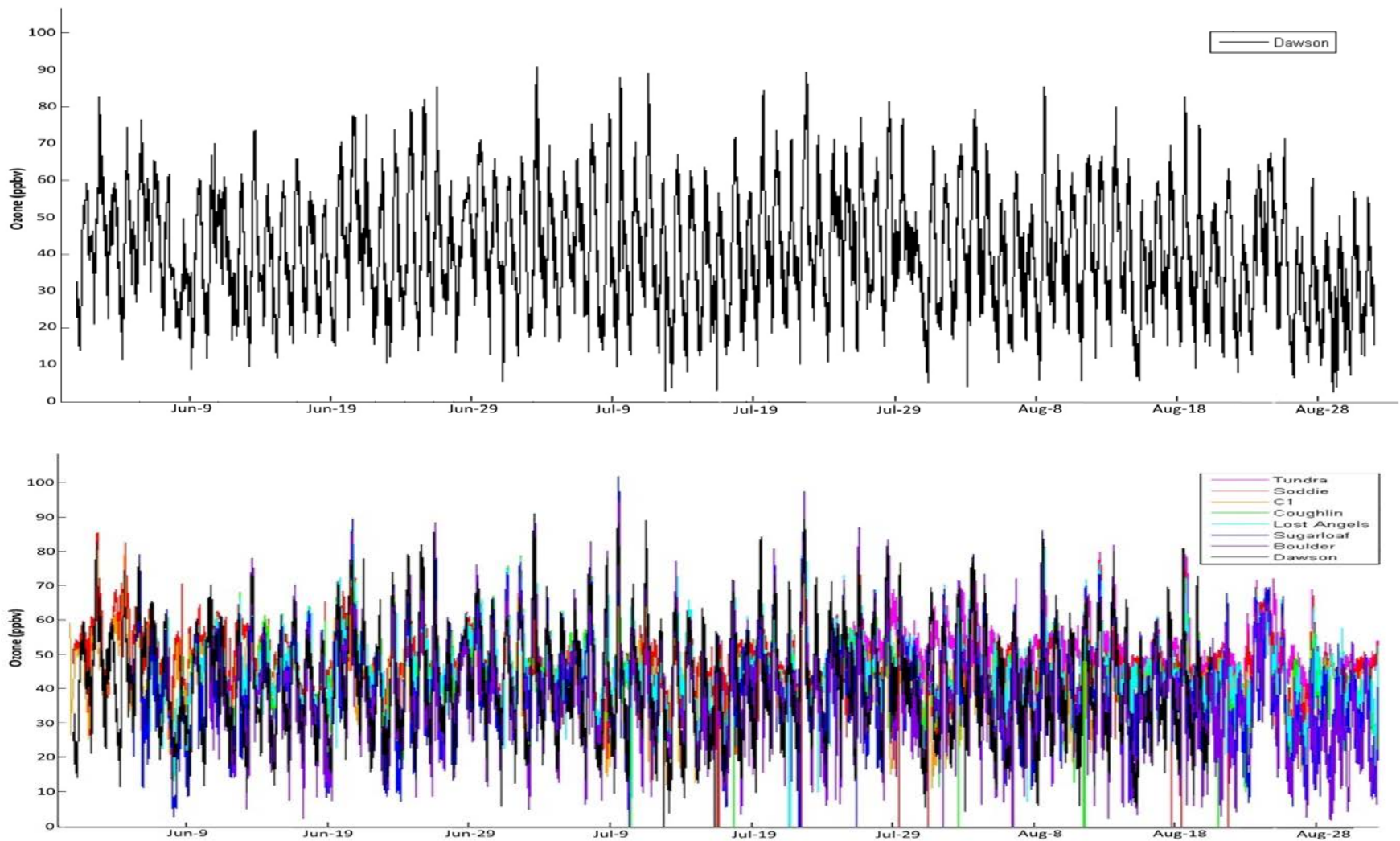


Figure 13a Ozone measured at Dawson School (top) during summer 2014 and compared to summer observations from seven other sites that were operated in the context of the Colorado Front Range Air Pollution and Photochemistry Experiment (FRAPPE) along an elevation gradient from Boulder to the Colorado Continental Divide/CU Boulder Mountain Research Station (bottom). Displayed data are 5-min resolution measurement, except for Tundra, which is 1 hr.

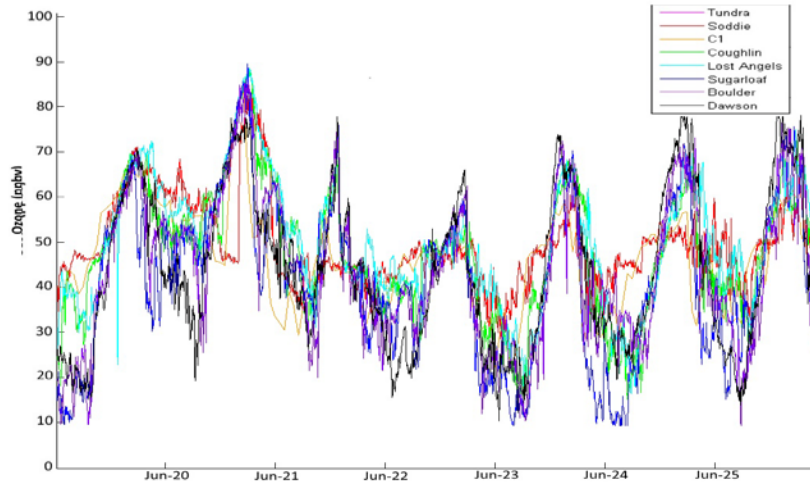
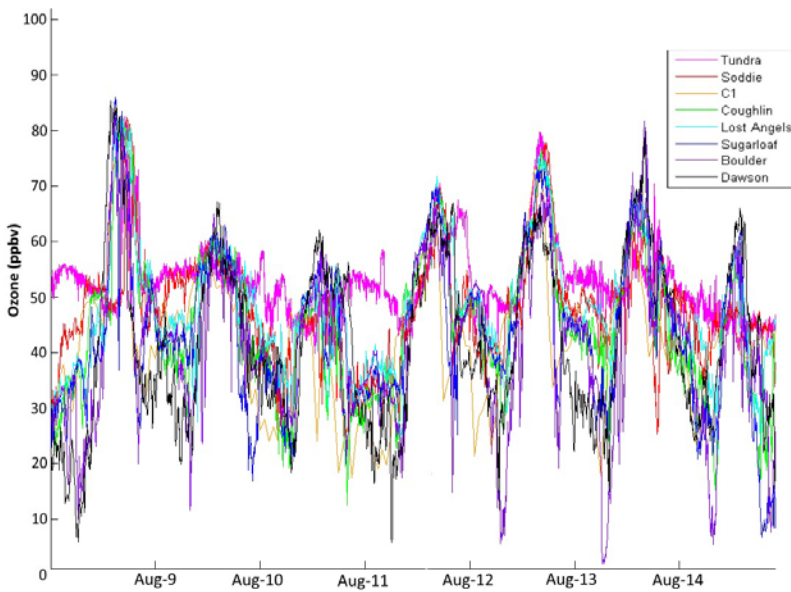
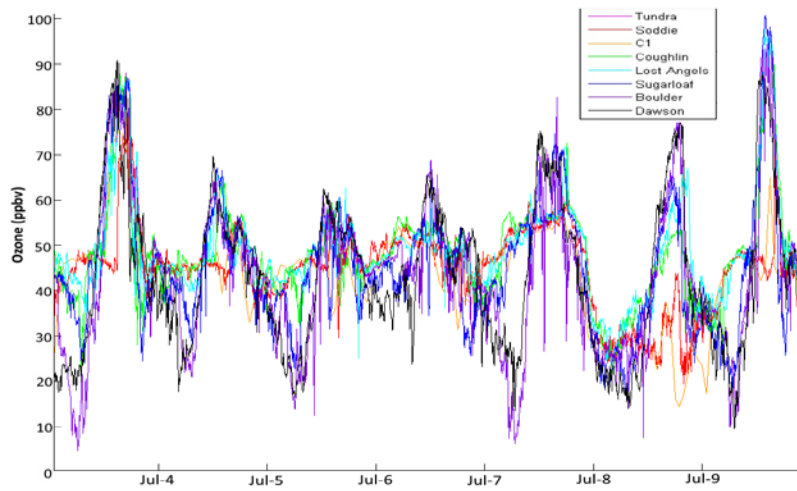
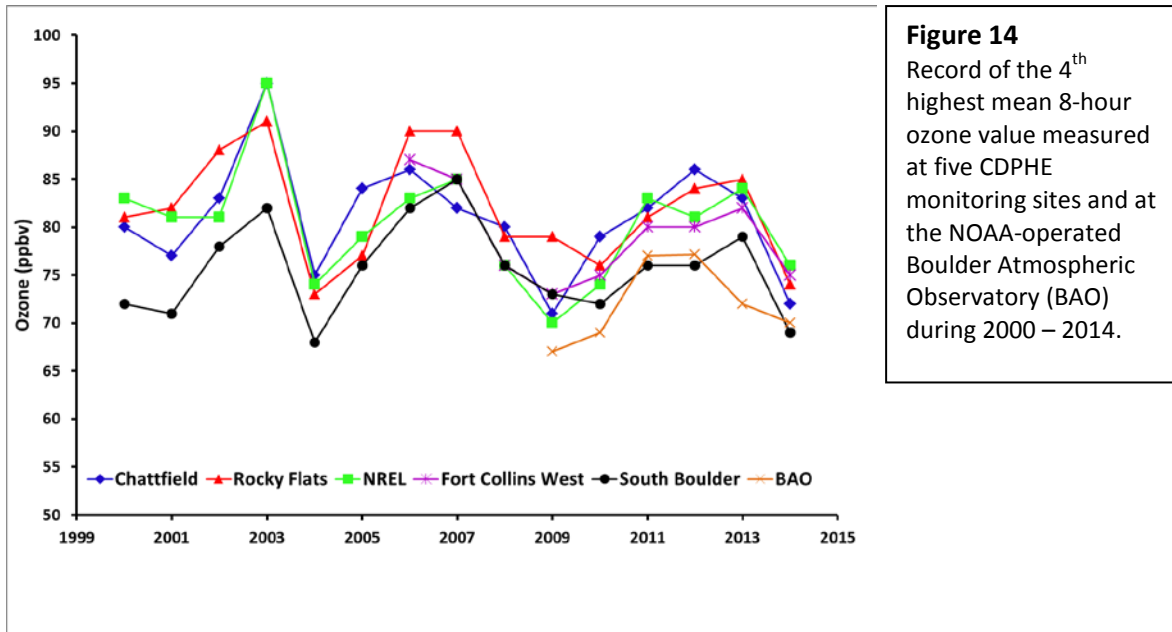


Figure 13b
1-week
enlargement of
selected
episodes of the
data in Figure
13a.





Methane measured by the five study sites by canister sampling and gas chromatography

Results for methane from the canister samples collected at each site are depicted in Figure 15. There was a significant degree of variability in the data between measurement days, which mostly is driven by atmospheric mixing and transport conditions on particular sampling days. Therefore, here we used box whisker plot to show the statistical distribution of measured values for a better comparison between sites. The atmospheric background during the 2014 summer was approximately 1.87 ppm (value derived from NOAA measurements conducted at Niwot Ridge), shown as a red horizontal line in the figure. Methane was lowest at the BCPH site. Levels increased towards the east of the county, and highest levels were observed at Stephen Day Park in Longmont. The measured values above background in Longmont were approximately twice those seen in Boulder. There was a noticeable increase in variability with increasing absolute levels, indicated by the wider spread of the data at the eastern monitoring sites. These two features (higher absolute levels as well as higher variability) are a clear indication of higher abundance and stronger strength of methane sources in the eastern part of the county, respectively toward the eastern county boundaries.

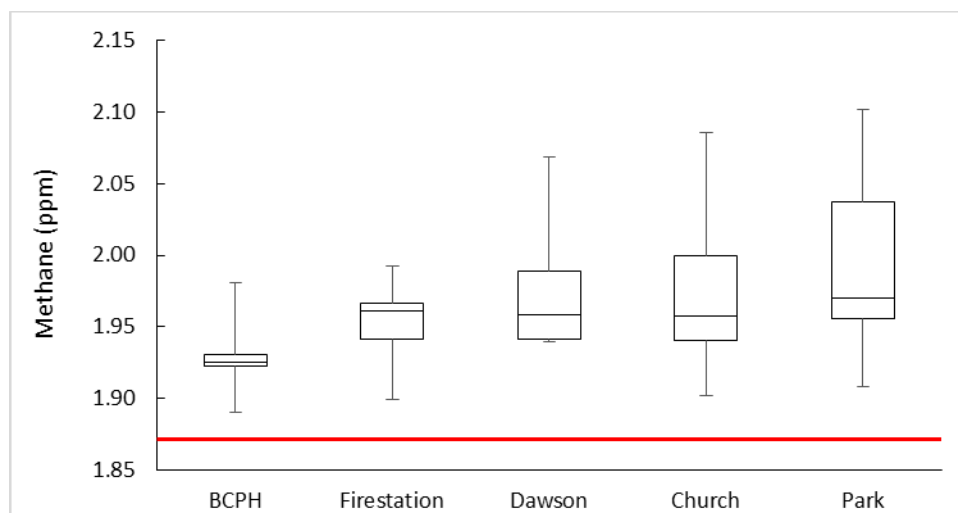


Figure 15

Box whisker plots showing the statistical distribution of methane in 3-day integrated canister samples collected at the five study sites. Each box whisker was derived from 9-11 individual measurements. The upper and lower borders of the boxes show the 25 and 75 percentile of the data, the horizontal line in the center the median, and the whiskers depict the minima and maxima. The red line shows the approximate background level of methane (1.87 ppm) during summer 2014.

VOC measured at the five study sites

A first look at the VOC data distribution in Figure 9 shows that there were generally higher levels seen at the eastern County sites for the O&NG associated VOC, while for other VOC this pattern was not as evident. Analyzing all 2014 canister VOC data in box whisker plot format further underscores this pattern (Figure 16). The light alkanes show a distinct increase in atmospheric mole fractions moving from Boulder towards the eastern sites, while other compounds with mixed sources including transportation-related emissions (alkenes, aromatic compounds) show a similar distribution among sites. Benzene falls in the latter group with similar distribution across sites. Besides absolute mole fractions increasing towards the eastern sites there also is an obvious increase in the variability or spread of encountered mole fraction, which can be interpreted as an indication that elevated VOC levels at these sites are driven by strong selected point sources rather than uniformly distributed.

VOC results are plotted against methane in Figure 17 to investigate their correlation. This comparison shows that results vary by compound. For the light n-alkanes, many of the samples elevated levels of VOC correlate with elevated methane, and there is a clear tendency of both having elevated levels at the eastern sites. This relationship is much weaker, respectively absent for alkenes and aromatic compounds. This behavior suggests that both methane and the light n-alkanes share common sources, while other VOC sources are likely more diverse.

VOC levels observed in this study were below currently set acute or chronic exposure thresholds. It should be noted, though, that these thresholds do not consider life-long exposure and the synergetic effects of exposure to multiple species together at the same time. Several recent studies have questioned currently applied exposure assessment criteria and called for more thorough investigation of VOC exposure limits and revisiting of health thresholds (McKenzie et al., 2012; Colburn et al., 2013;

McKenzie et al., 2015). Benzene levels at all sites ranged between 0.2 – 1.2 ppbv (25-75 percentile range). Lifetime exposure to $1.7 \mu\text{g m}^{-3}$ (~ 0.5 ppb) of benzene increases the risk of cancer to 1 in 100,000 (WHO, 2010; EPA, 2013). In evaluating these data it needs to be considered that these are summer observations, when ambient VOC tend to be lowest. Consequently, year-round average values are anticipated to be higher than the values determined in this summer study. Results from this study showed levels above respectively very close to the WHO exposure threshold at all sites. Several other previous studies (Pétron et al., 2012; Swarthout et al., 2013; Thompson et al., 2014) have shown that oil and gas operations are a major source of benzene and other BTEX compounds in the Colorado Front Range. There are multiple sources contributing to BTEX emissions, with mobile sources (automobiles) likely being one of the major ones. Oil and gas associated emission likely have an increasing contribution in the eastern part of Boulder County.

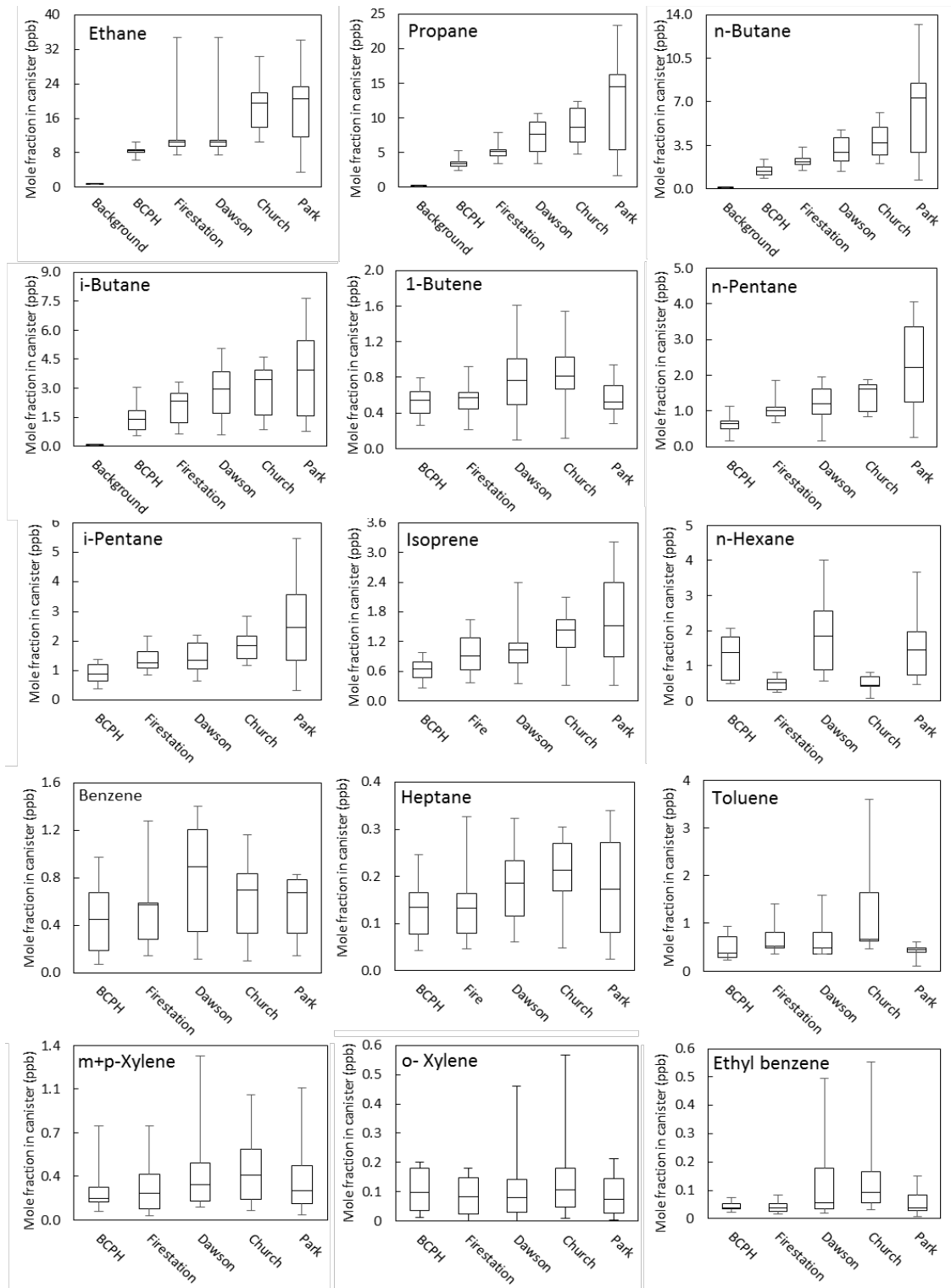


Figure 16

Statistical distribution of VOC ambient mole fractions among sites. These box-whiskerplots show the median mole fractions by the horizontal line in the middle, the 25-75 percentile of data by the upper and lower box boundaries, and the minima and max by the end points of the vertical lines. The 'Background' data reflect levels that would be seen outside and upwind of the urban corridor.

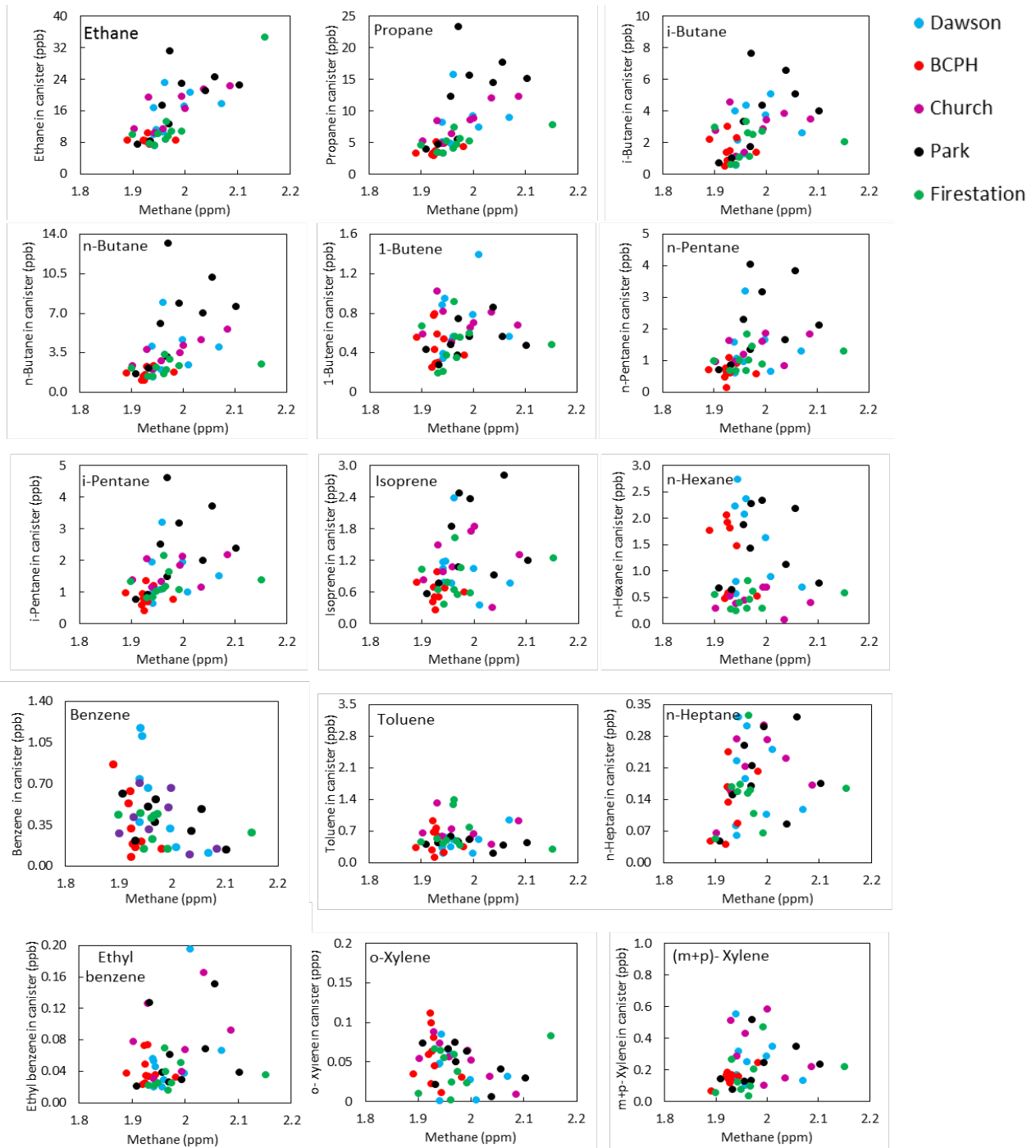


Figure 17

Relationship between methane and VOC in the Summa canister samples collected at the five study sites. The correlations seen in the data suggest that emissions of these NMHC are primarily associated with methane emission sources. Elevated levels of both compounds classes are seen at the eastern County sites.

References

- Brodin M, Helmig D, Oltmans S. 2010. Seasonal ozone behavior along an elevation gradient in the Colorado Front Range Mountains. *Atmospheric Environment* 44(39):5305-5315. doi:10.1016/j.atmosenv.2010.06.033.
- Colburn T, Schultz K, Herrick L, Kwiatkowski C. 2013. An exploratory study of air quality near natural gas operations. *Human and Ecological Risk Assessment: An International Journal* doi.org/10.1080/10807039.2012.749447.
- Eisele A, Hannigan M, Milford J, Helmig D, Milmoie P. 2008. Understanding Air Toxics and Carbonyl Pollutant Sources in Boulder County, Colorado. *Environmental Protection Agency* <http://www.epa.gov/ttnamti1/files/20052006csatam/BCPHAirToxicsReportEPA.pdf>: Accessed December 29, 2014.
- EPA. 2013. Integrated Risk Information System (IRIS): Benzene Summary. *Environmental Protection Agency* <http://www.epa.gov/iris/sust/O276.htm>: Accessed December 29, 2014.
- McKenzie LM, Witter RZ, Newman LS, Adgate JL. 2012. Human health risk assessment of air emissions from development of unconventional natural gas resources. *Science of the Total Environment* 424:79-87. doi:10.1016/j.scitotenv.2012.02.018.
- McKenzie LM, Guo R, Witter RZ, Savitz DA, Newman LS, et al. 2015. Birth outcomes and maternal residential proximity to natural gas development in rural Colorado. *Environmental Health Perspectives* <http://dx.doi.org/10.1289/ehp.1306722>.
- Pétron G, Frost G, Miller BR, Hirsch AI, Montzka SA, et al. 2012. Hydrocarbon emissions characterization in the Colorado Front Range: A pilot study. *Journal of Geophysical Research-Atmospheres* 117:1-19. doi:10.1029/2011jd016360.
- Swarthout RF, Russo RS, Zhou Y, Hart AH, Sive BC. 2013. Volatile organic compound distributions during the NACHTT campaign at the Boulder Atmospheric Observatory: Influence of urban and natural gas sources. *Journal of Geophysical Research-Atmospheres* 118(18):10614-10637.
- Thompson CR, Hueber J, Detlev H. 2014. Influence of oil and gas emissions on ambient atmospheric non-methane hydrocarbons in residential areas of Northeast Colorado. *Elementa* 2:1-16. doi:10.12952/journal.elementa.000035.
- WHO. 2010. Exposure to Benzene: A Major Public Health Concern. *World Health Organization* <http://www.who.int/ipcs/features/benzene.pdf>: Accessed December 29, 2014.

Final Report – OG Pod Section

Air Quality Monitoring Study to Assess Exposure to Volatile Organic Compounds and Develop Cost-Efficient Monitoring Techniques

Prepared and submitted by:

Detlev Helmig, INSTAAR, Univ. of Colorado

Mike Hannigan, Mechanical Engineering, Univ. of Colorado

Jana Milford, Mechanical Engineering, Univ. of Colorado

Joanna Gordon, Mechanical Engineering, Univ. of Colorado

May 13, 2015

OG-Pod Section Contents

Introduction

Methods

- Summary Of Measurements
- Sensors
- Description Of Calibration and Quantification Methods
 - Flow Chart Showing Calibration Process
 - Ozone Calibration Example
- Calibration Model Attributes

Results

Ozone

- Comparison Of INSTAAR Ozone and Pod BE Ozone At Dawson School
- Ozone Model Parameter Space and Discussion Of Observed Ozone NAAQS Exceedances:
- Comparison Of Ozone From Two Pods Co-Located At Dawson School: Pod BE and Pod N3 (Pod N3 Was Deployed For One Month During FRAPPE, Co-Located With Pod BE During That Time.)
- Ozone Correlation At Dawson School, The Lafayette Fire Station, and St. Luke's Church
- Weekly Hour Averaged Ozone Dawson School, The Lafayette Fire Station, and St. Luke's Church

Methane

- Methane Calibration Functions
- Parameter Space Comparison For Methane Co-Location and BC Data: Temperature and Relative Humidity

Discussion

OG-Pod Monitoring Guidelines

Appendix:

- Sensor Principles of Operation
- Methane Calibration Functions
- Weekly Plots Showing Hour Averaged Ozone

Introduction:

In recent years, the Hannigan Research Group at CU Boulder has been working to develop low-cost, easy-operable air quality monitors. These air quality monitors, called Pods, contain sensors that respond to various atmospheric trace gases. The sensors included in each Pod can be selected to accommodate specific projects or questions. For this study, in which one of the objectives is to investigate how an air shed near a large oil and gas production region could be impacted by the industry, and compare the Pod performance to traditional air quality monitoring techniques, we constructed five pods with sensors that respond to gases of interest in this context. We termed these five air monitors “OG-Pods”, short for Oil and Gas Pods. Herein, they will be referred to as Pods and OG-Pods interchangeably.

The status quo for gas phase air quality monitoring instruments with high time resolution is expensive (\$5,000 - \$100,000 per single gas). A Pod, which can measure multiple gases with high resolution in time, costs only about \$1,000. Pods use less power than the status quo gas monitors, and don't need a climate controlled structure to house them in the field, as they are enclosed in weather-proof housing. Rather than relying on a pump to pull air through an optical cavity at a fixed rate, Pods use a fan to continually bring outside air inside the enclosure, and into contact with the sensors housed inside.

Pods provide an alternative air quality monitoring platform, with many advantages over the status quo, but this new technology does pose challenges. Calibration, sensor signal quantification, and assessment of data quality are all non-trivial. Our efforts to better translate sensor signal into a meaningful concentration or mole fraction are ongoing and a focal point in this report.

Methods

The sensors:

The OG-Pods constructed for this study were equipped with sensors that respond to the following gases in the air: Ozone (O_3), Methane (CH_4), Total Volatile Organic Compounds (Total VOCs), Nitrogen Dioxide (NO_2), Nitric Oxide (NO), Carbon Monoxide (CO), and Carbon Dioxide (CO_2). Each Pod also contained temperature and humidity sensors. Three of the Pods deployed in this study were set up to log wind speed and direction in addition. Pods log a voltage signal from each of these sensors approximately every 10 seconds, when the data is written to a text file, and stored on a micro-SD card. Each gas sensor in an OG-Pod operates on one of three physical principles, which are described below.

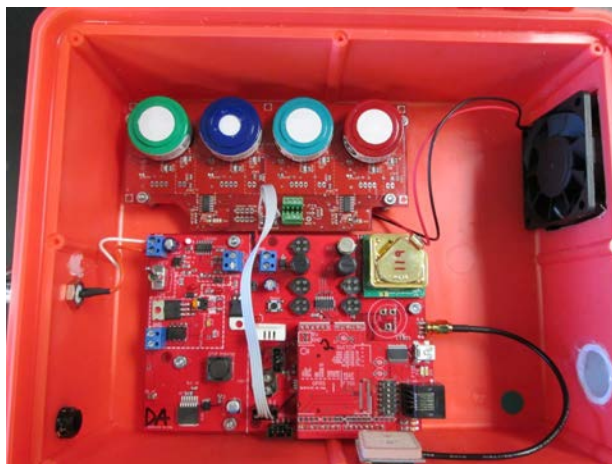


Figure 18: An inside view of a Pod.

Gas		Sensor Type	Manufacturer	Model
Ozone	O ₃	Metal Oxide	SGX (Formerly E2V)	MICS-2611
Methane	CH ₄	Metal Oxide	Figaro	2600
Volatile Organic Compounds	Total VOCs	Metal Oxide	Figaro	2602
Nitrogen Dioxide	NO ₂	Metal Oxide	SGX (Formerly E2V)	MICS-2710
Nitric Oxide	NO	Electrochemical	Alphasense	NO-B4
Carbon Monoxide	CO	Metal Oxide	SGX (Formerly E2V)	MISC-5525
Carbon Dioxide	CO ₂	Non-Dispersive Infrared	ELT	s300

Table 1: The table above shows information on the sensor used in the OG-Pods during the study. Refer to the appendix for an explanation of the physical principles of operation for each sensor type.

Calibration:

We have seen the best sensor signal quantification results via co-location calibration. While the sensors in the Pods do respond to the gases we are interested in measuring, they also respond to changing environmental parameters such as temperature and humidity. It is difficult to simulate this changing environmental parameter space during a lab calibration, so instead, we calibrate outside, where this parameter space changes naturally.

We co-locate our Pods with regulatory air monitoring equipment (or instruments of similar caliber), which is to say, that we position our Pods so they are sampling the same air the well-trusted instruments are sampling. During this study, we used the Colorado Department of Health and Environment (CDPHE) air quality monitoring site in downtown Denver, CAMP, as our co-location calibration site. In an effort to encompass a relatively wide range of gas concentrations, temperatures, and humidity, we generally allow about one week per co-location calibration. Over the summer of 2014, we ran four, week-long, co-location calibrations at CAMP, at a frequency of approximately one calibration per month. CDPHE supplied us with the one minute-averaged data from their regulatory air monitoring instruments for the following gases: O₃, NO, NO₂, and CO. We refer to the data from these regulatory grade air quality monitors as reference measurements.

We set up a calibrated Licor CO₂ analyzer (LI-840A CO₂/H₂O) there ourselves so we could calibrate for CO₂ as well as the species that CDPHE monitors during each calibration. There was, however, an unexpected data logging issue with the Licor we set up, so only one calibration for CO₂ was generated. For this calibration, the time stamp from the Licor CO₂ analyzer was reconstructed based on the sensor signal trend. We didn't have a way to calibrate the total VOC sensor signal. The raw sensor signal data is available upon request.



Figure 19: This is a photo of CDPHE's CAMP air quality monitoring site in downtown Denver. This site was used for co-location calibrations for the Pods. Picture Source: Ashley Collier

In general, after a co-location calibration, we calculate one-minute averages for our sensor signals so the Pod data are on the same time resolution as the reference measurements. We then convert each sensor voltage into a resistance. We then divide by a baseline resistance, specific to each sensor, which we refer to as r_0 . This new metric, r/r_0 , is then used as the sensor signal moving forward. We run a multiple linear regression model, using sensor signal, temperature, and relative humidity, as predictors of the reference signal. With this model is an equation that gives a mole fraction of each gas species as a function of sensor signal, temperature, and relative humidity. We can then apply this equation to Pod data at measurements sites.

For this study, the co-location calibration data were taken from the calibration period before and after approximately each month of data collection. We generated a calibration equation using multiple linear regressions. The calibration equation was then applied to the data collected between the two surrounding calibration periods. The sensors tend to drift in time, so calibrating on a monthly basis addressed issues with sensor drift. In addition, by calibrating on a monthly basis, we aimed to encompass current environmental parameters (gas mole fractions, temperature, and humidity space) in our models. For example, July is generally warmer and more humid than May, so a calibration generated in May would not encompass a wide enough range of temperature or humidity for July field measurements.

At the Dawson School site, the INSTAAR Team operated a Thermo Environmental Instruments Model 49 Ozone Analyzer, which was co-located with one of the OG-Pods from June through September. The ozone data from this instrument is used to help evaluate the pod ozone data on location at a project air quality measurement site.

The figure below shows the general process of translating a raw sensor signal into a concentration, or a mole fraction for a given gas species. As soon as mole fraction, temperature, or humidity leave our model's parameter space, we are extrapolating, which is not ideal. Our calculated uncertainty no longer stands.

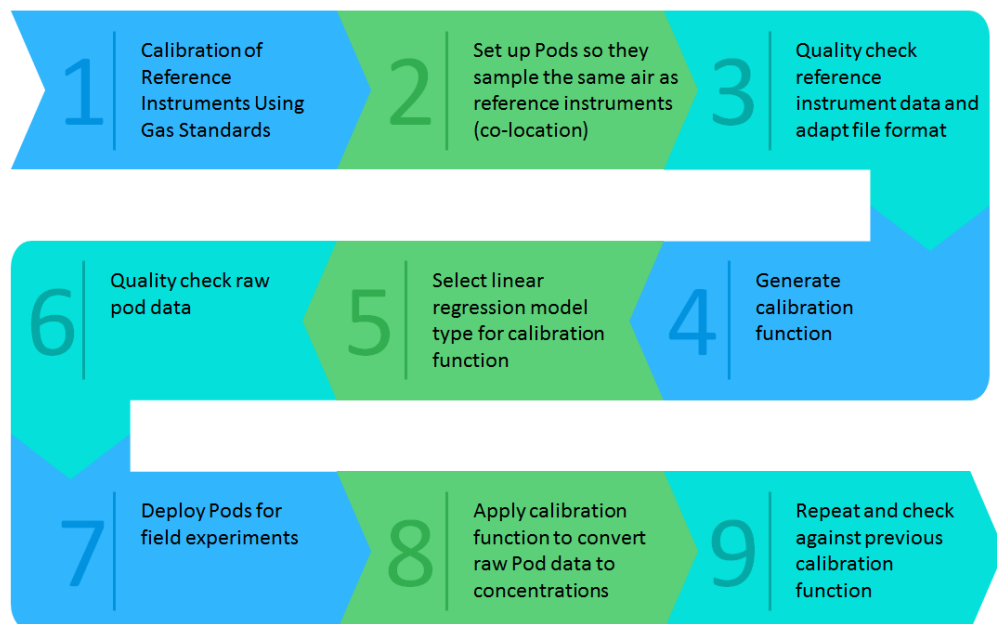


Figure 20: This flowchart details the process of converting the raw sensor signals from the OG-Pods into mole fractions.

The figure below shows an example of a linear model for ozone, where sensor signal, temperature, and relative humidity are used as predictors toward reference data from CAMP. The blue line shows CAMP data, and the red line shows the linear model, denoted “CAMP Cal4” because it was the fourth calibration period of the summer. The 95% confidence interval of the linear model is plotted in green.

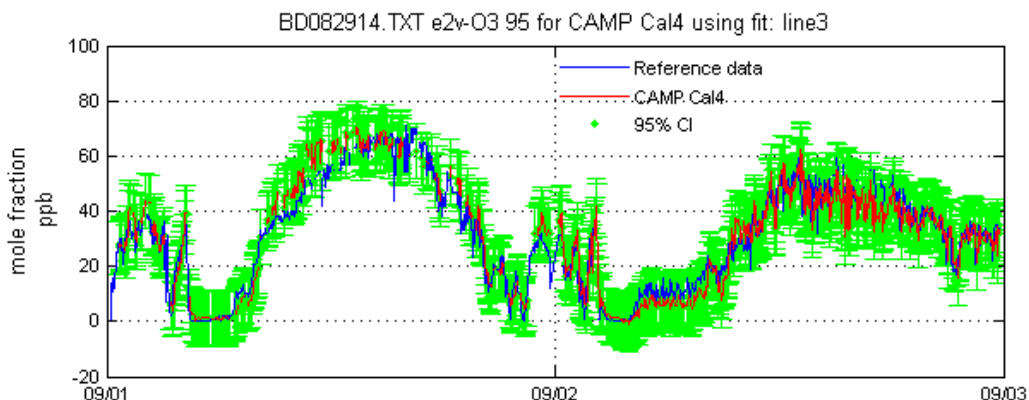


Figure 21: This ozone plot shows in red, a linear model’s agreement with ozone data from CAMP, which is termed Reference data and shown in blue. The green bars represent the 95% confidence interval for the linear model. The model’s root mean squared error is 4.22 ppb and the adjusted r^2 is 0.87.

Calibration Models

The signal-to-noise ratio is calculated as the mean mole fraction of a gas species during calibration divided by the root mean squared error of the model generated from that calibration data. A high signal-to-noise ratio makes for a useful model. If a signal to noise ratio drops below two, the noise begins to drown out observable trends in the data, and the calibration does not yield useful information. Related to the signal-to-noise ratio, is the root mean squared error (RMSE) associated with a model. A small RMSE indicates low uncertainty. The r^2 value indicates the percent of variability in the data that can be explained by the model. The adjusted r^2 value penalizes the r^2 according to the number of predictors used in the model. A large adjusted r^2 value indicates the trend in the data has been captured well by the model. The tables below show these attributes for each model. Three models were generated for each OG-Pod and for all of the species monitored at CAMP (ozone, carbon monoxide, nitric oxide, and nitrogen dioxide). One model was generated for four of the OG-Pods, in July for carbon dioxide. As far as ozone linear regression models are concerned, an r^2 of 0.8 or greater is acceptable, and an r^2 of 0.9 or better is very good. The root mean squared error associated with an ozone model is generally smaller than 5 ppb.

Tabulated values for methane calibration signal to noise ratios are included because we gained access to a methane reference instrument for a post-sampling period calibration in November. The methane reference instrument was housed in a mobile lab. It was a Picarro cavity ring-down methane analyzer. The calibrations look promising, but as will be discussed in the results section of the report, the parameter space from the November calibration poorly matches that of summer in terms of temperature and relative humidity, so these models are not used to quantify methane during the summer study. Attributes of carbon dioxide models are also included from the third calibration period at CAMP. Please note that the signal to noise ratio for carbon dioxide is highest, methane and ozone are on the order of 7 - 11, and the rest are appreciably smaller. Using measures like the signal to noise ratio, we are continually assessing the quality of our data for each sensor calibration. Some calibrations are better than others. We expect there to be changes in this parameter in time, because the signal and

environmental parameters are changing in time. For example, since some months have higher ozone, we can expect a better signal to noise ratio with the same root mean squared error in the calibration model. Additionally, two calibrations for the same sensor could yield different root mean squared errors, which would also affect this parameter. We expect it to change, and we are careful to assess each model individually. In general the signal to noise ratios we see for the methane and ozone sensors are sufficient to see trends in the data. The signal to noise ratio for nitrogen dioxide and carbon monoxide are between one and two, and this metric is less than one in the case of nitric oxide. Because these three species have such small signal to noise ratios, there is very large uncertainty in the measured magnitudes of their mole fractions, and so they are not included in the official report. Plots showing these data are available upon request.

However, the general trend for nitrogen dioxide, in particular, seems to demonstrate some explanatory power with regard to ozone in some cases. For example, in many cases ozone dips down lower at the Stephen Day Park site in Longmont than at all the other sites. The NO₂ trend at the Stephen Day Park site is higher than at all other sites in a number of these instances. Because NO₂ removes ozone at night, these observed trends in ozone and NO₂ are plausible. In general, we have had better success measuring CO and NO_x in winter months when concentrations at CAMP are larger, and we can achieve better signal to noise ratios with our models. The Licor carbon dioxide analyzer we were running at CAMP throughout the summer had some unforeseen data logging issues, and as a result there was only one calibration period for carbon dioxide. This one co-location calibration for carbon dioxide relies on a re-constructed time stamp for the Licor CO₂ data, which was estimated by examination of patterns in CO₂. Due to limitations of the data available for calibrating the CO₂ sensors, these measurements are also excluded from this report, but are available upon request. With that, the results presented below focus primarily on the ozone data, together with limited results for CH₄ that should be interpreted as preliminary proof of concept information for the utility of the Pods in measuring this pollutant.

Ozone:

Cal1 - Cal2	Deployment Site	Adjusted r ²	Root Mean Squared Error (ppb)	Signal to Noise Ratio
Pod BA	Fire Station	0.92	3.8	9.45
Pod BB	Steven Day Park	0.85	4.8	7.48
Pod BD	BC Public Health	0.91	3.9	9.21
Pod BE	Dawson School	0.91	3.9	9.21
Pod BF	St. Luke Church	0.91	3.1	11.58
Cal2 - Cal3	Deployment Site	Adjusted r ²	Root Mean Squared Error (ppb)	Signal to Noise Ratio
Pod BA	Fire Station	0.91	3.2	10.81
Pod BB	Steven Day Park	0.74	4.2	8.24
Pod BD	BC Public Health	0.9	3.6	9.61
Pod BE	Dawson School	0.9	3.5	9.89
Pod BF	St. Luke Church	0.88	3.9	8.87
Cal3 - Cal4	Deployment Site	Adjusted r ²	Root Mean Squared Error (PPB)	Signal to Noise Ratio
Pod BA	Fire Station	0.86	3.6	8.14
Pod BB	Steven Day Park	0.87	3.7	7.92
Pod BD	BC Public Health	0.89	4.3	6.81
Pod BE	Dawson School	0.86	3.7	7.92
Pod BF	St. Luke Church	0.89	3.7	7.92

Table 2: Linear model attributes for ozone.

CH4:

Post-Cal	Deployment Site	Adjusted r^2	Root Mean Squared Error (ppm)	Signal to Noise Ratio
Pod BA	Fire Station	0.62	0.31	7.62
Pod BB	Steven Day Park	0.72	0.35	6.75
Pod BD	BC Public Health	0.75	0.29	8.15
Pod BE	Dawson School	0.72	0.3	7.88
Pod BF	St. Luke Church	0.67	0.2	11.81

Table 3: Linear model attributes for methane.

CO2:

Cal3	Deployment Site	adjusted r^2	Root Mean Squared Error (ppm)	Signal to Noise Ratio
Pod BA	Fire Station	0.76	15	31.53
Pod BD	BC Public Health	0.46	19	24.89
Pod BE	Dawson School	0.56	18	26.28
Pod BF	St. Luke Church	0.88	14	33.79

Table 4: Linear model attributes for carbon dioxide.

NO2:

Cal1 - Cal2	Deployment Site	Adjusted r^2	Root Mean Squared Error (ppb)	Signal to Noise Ratio
Pod BA	Fire Station	0.54	13	1.14
Pod BB	Steven Day Park	0.55	11	1.35
Pod BD	BC Public Health	0.54	12	1.23
Pod BE	Dawson School	0.56	12	1.23
Pod BF	St. Luke Church	0.54	11	1.35
Cal2 - Cal3	Deployment Site	Adjusted r^2	Root Mean Squared Error (ppb)	Signal to Noise Ratio
Pod BA	Fire Station	0.3	11	1.64
Pod BB	Steven Day Park	0.36	8.9	2.02
Pod BD	BC Public Health	0.28	12	1.50
Pod BE	Dawson School	0.34	10	1.80
Pod BF	St. Luke Church	0.29	11	1.64
Cal3 - Cal4	Deployment Site	Adjusted r^2	Root Mean Squared Error (ppb)	Signal to Noise Ratio
Pod BA	Fire Station	0.29	13	1.41
Pod BB	Steven Day Park	0.37	9	2.04
Pod BD	BC Public Health	0.29	12	1.53
Pod BE	Dawson School	0.33	12	1.53
Pod BF	St. Luke Church	0.27	13	1.41

Table 5: Linear model attributes for nitrogen dioxide.

NO:

Cal1 - Cal2	Deployment Site	Adjusted r^2	Root Mean Squared Error (PPB)	Signal to Noise Ratio
Pod BA	Fire Station	0.73	11	0.79
Pod BB	Steven Day Park	0.66	26	0.33
Pod BD	BC Public Health	0.57	13	0.66
Pod BE	Dawson School	0.79	14	0.62
Pod BF	St. Luke Church	0.83	16	0.54
Cal2 - Cal3	Deployment Site	Adjusted r^2	Root Mean Squared Error (PPB)	Signal to Noise Ratio
Pod BA	Fire Station	0.85	12	0.62
Pod BB	Steven Day Park	0.79	19	0.39
Pod BD	BC Public Health	0.73	20	0.37
Pod BE	Dawson School	0.68	37	0.20
Pod BF	St. Luke Church	0.74	15	0.49
Cal3 - Cal4	Deployment Site	Adjusted r^2	Root Mean Squared Error (PPB)	Signal to Noise Ratio
Pod BA	Fire Station	0.6	21	0.49
Pod BB	Steven Day Park	0.52	83	0.12
Pod BD	BC Public Health	0.6	21	0.49
Pod BE	Dawson School	0.57	18	0.57
Pod BF	St. Luke Church	0.67	25	0.41

Table 6: Linear model attributes for nitric oxide.

CO:

Cal1 - Cal2	Deployment Site	Adjusted r^2	Root Mean Squared Error (ppm)	Signal to Noise Ratio
Pod BA	Fire Station	0.72	0.14	1.62
Pod BB	Steven Day Park	0.85	0.16	1.42
Pod BD	BC Public Health	0.45	0.14	1.62
Pod BE	Dawson School	0.4	0.15	1.51
Pod BF	St. Luke Church	0.96	0.2	1.14
Cal2 - Cal3	Deployment Site	Adjusted r^2	Root Mean Squared Error (ppm)	Signal to Noise Ratio
Pod BA	Fire Station	0.2	0.22	1.32
Pod BB	Steven Day Park	0.44	0.19	1.53
Pod BD	BC Public Health	0.21	0.21	1.38
Pod BE	Dawson School	0.19	0.22	1.32
Pod BF	St. Luke Church	0.21	0.17	1.71
Cal3 - Cal4	Deployment Site	Adjusted r^2	Root Mean Squared Error (ppm)	Signal to Noise Ratio
Pod BA	Fire Station	0.22	0.2	1.49
Pod BB	Steven Day Park	0.26	0.18	1.66
Pod BD	BC Public Health	0.38	0.17	1.76
Pod BE	Dawson School	0.34	0.18	1.66
Pod BF	St. Luke Church	0.32	0.14	2.14

Table 7: Linear model attributes for carbon monoxide.

Results

Ozone

Comparison of INSTAAR Ozone and Pod BE Ozone Measurements at Dawson School:

The figure below shows five-minute ozone data acquired by a pod and a reference instrument run by the INSTAAR team at the Dawson School study site. The magenta line indicates what a 1:1 relationship would look like, and the linear regression line is shown in red. In general, the Pod gives slightly higher values for ozone than the INSTAAR reference instrument. This trend becomes less pronounced with increased mole fraction, until the two lines cross.

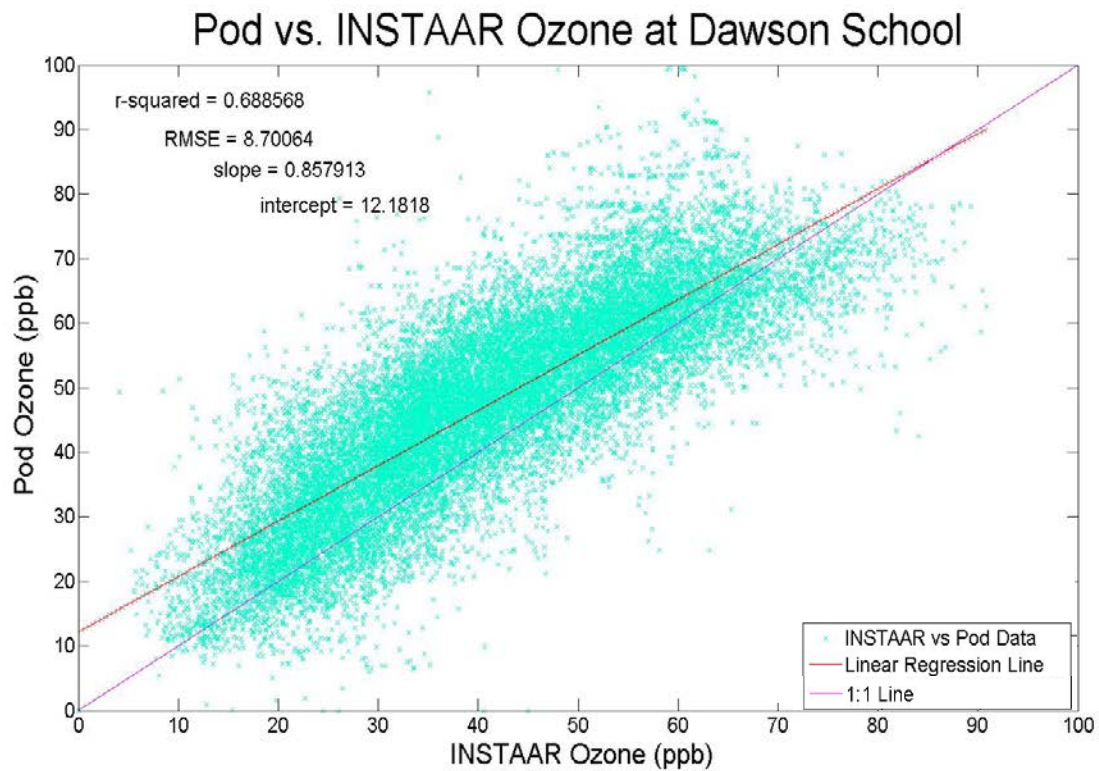


Figure 22: Five-minute resolution ozone measurements from Pod BE and INSTAAR monitor at the Dawson School site.

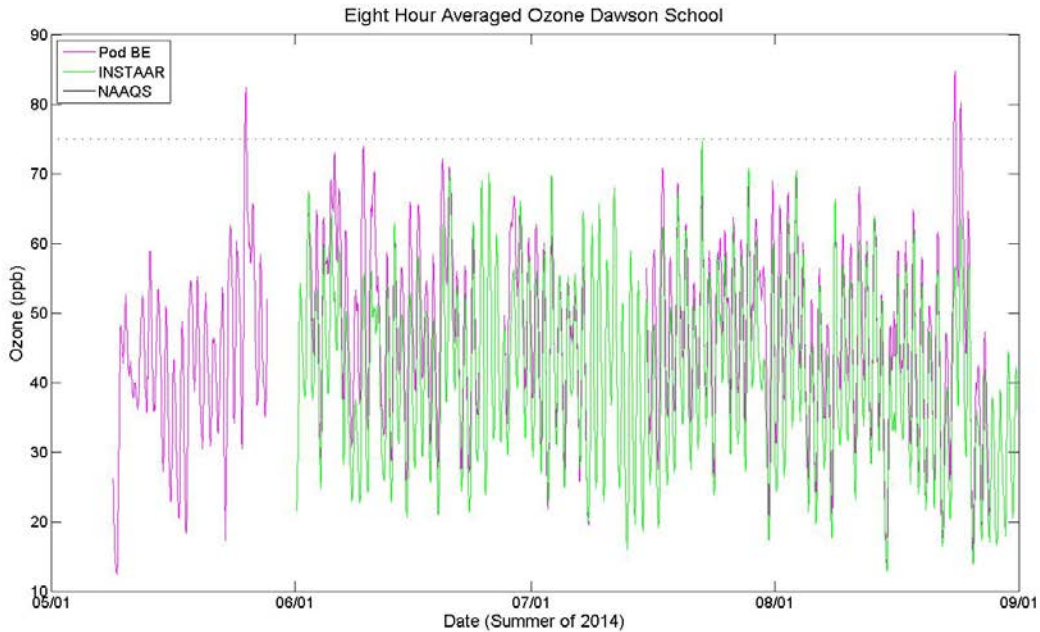


Figure 23: This time series shows how the eight-hour average Pod and INSTAAR ozone measurements at Dawson School compare.

The above figure compares the eight hour-averaged data at Dawson School for Pod BE and the INSTAAR ozone reference instrument. Both data sets were first averaged on an hourly basis and then averaged on a rolling eight-hour basis. This averaging structure is similar to the system used in determination of NAAQS exceedances. The hourly-averaged data used here did not start on the hour, however, as would need to be the case in order to address regulatory standards for the NAAQS, so this data differs from the regulatory method in that respect.

Pod BE recorded one exceedance of 75 ppb in May when the INSTAAR ozone reference monitor was not yet up and running. Pod BE recorded another spike above 75 ppb in late August, which was not corroborated by the INSTAAR reference monitor. To investigate why this disagreement among ozone measurements might occur, we plotted the ozone mole fraction parameter space for all of the observed ozone at the Boulder County study sites, and then overlaid the ozone mole fraction parameter space during each of the three calibration datasets from CAMP. These three plots can be found below.

All three CAMP distributions, shown in blue, encompass ozone mole fractions below about 60 ppb but fail to extend above this level. It follows that in the pod data from the Boulder County measurement sites, all mole fractions measured to be above about 60 ppb are extrapolated beyond the model calibration range. In order to get a higher quality measurement of ozone in the range of the NAAQS, and to estimate the uncertainty in such measurements, a calibration that encompassed higher ozone concentrations would be required.

Ozone Model Parameter Space

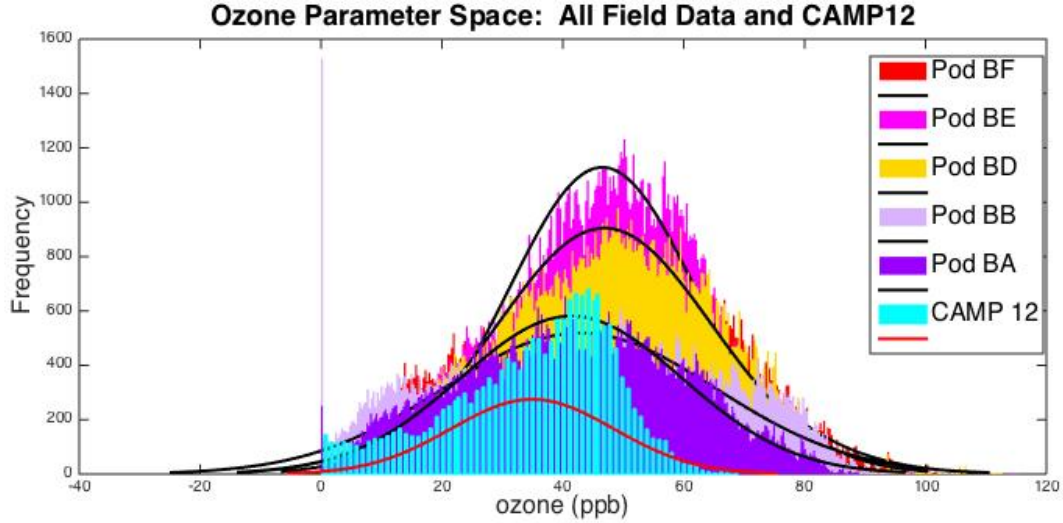


Figure 24: The plot above shows overlaid histograms of all the ozone data at the five study sites for all summer measurements. In front of all these, in blue, is a histogram that shows ozone from CAMP during the first two calibration periods. For the first portion of the summer measurements, a linear model based on this CAMP data was applied as a calibration function.

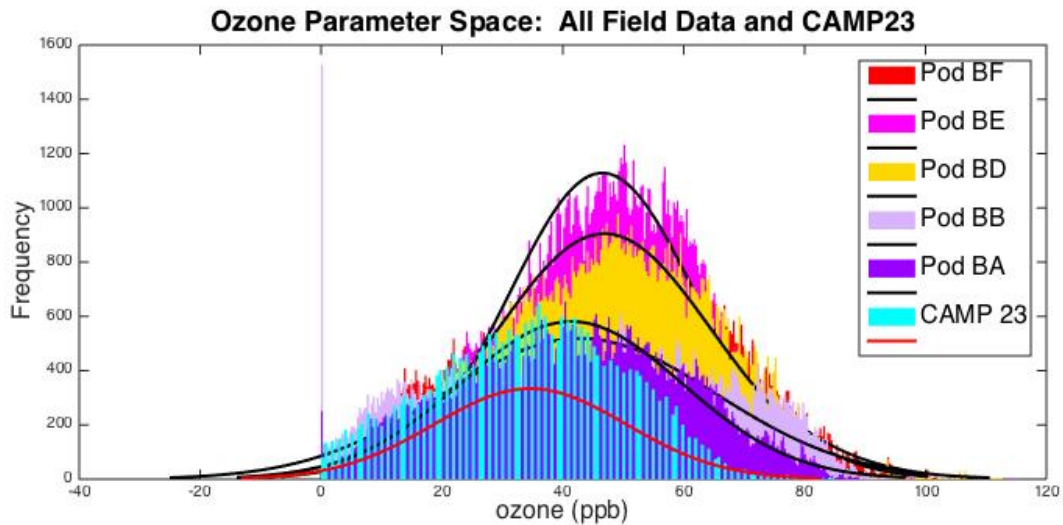


Figure 25: The plot above shows overlaid histograms of all the ozone data at the five study sites for all summer measurements. In front of all these, in blue, is a histogram that shows ozone from CAMP during the second and third calibration periods. For the second portion of the summer measurements, a linear model based on this CAMP data was applied as a calibration function.

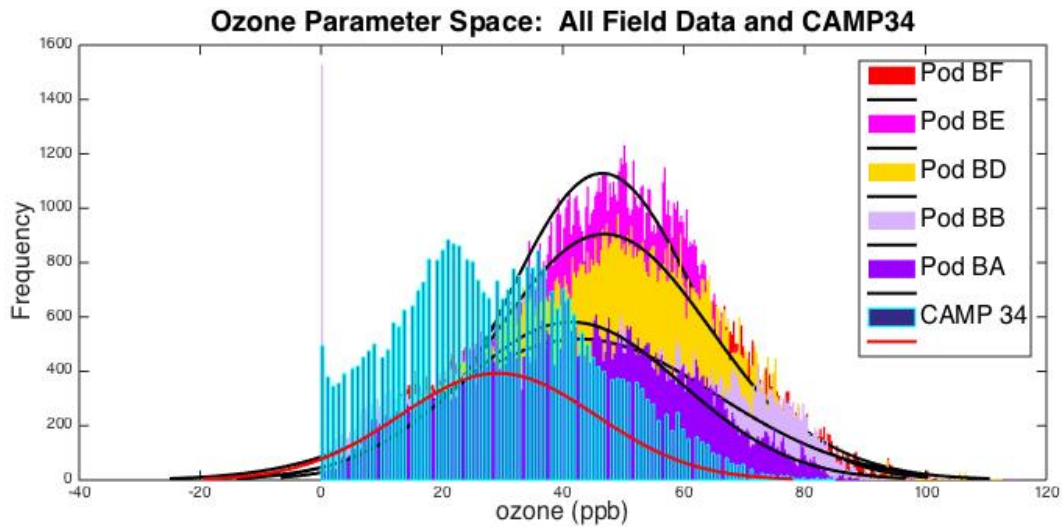


Figure 26: The plot above shows overlaid histograms of all the ozone data at the five study sites for all summer measurements. In front of all these, in blue, is a histogram that shows ozone from CAMP during the third and fourth calibration periods. For the last portion of the summer measurements, a linear model based on this CAMP data was applied as a calibration function.

Comparison of Pod BE Ozone and FRAPPE Pod Ozone Measurements at Dawson school:

The plots below show ozone data from two Pods that were co-located at the Dawson School study site. Pod BE was the Pod deployed at this site all summer for the Boulder County air quality research effort. Pod N3 was deployed at this site during the FRAPPE Campaign for about a month in July and August. Both plots show good agreement between the two Pods. In the second plot, the magenta line indicates a 1:1 relationship between the two measurements, and the red line shows a linear regression, with a slope very nearly equal to unity. This result supports good repeatability among measurements using Pods to monitor ozone.

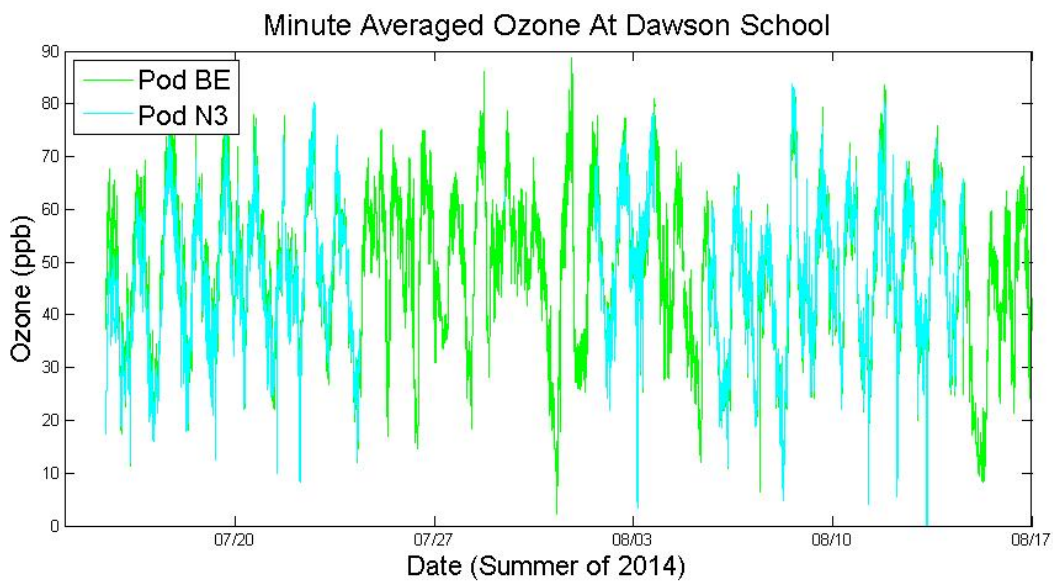


Figure 27: One minute average ozone data from two pods co-located at the Dawson school site.

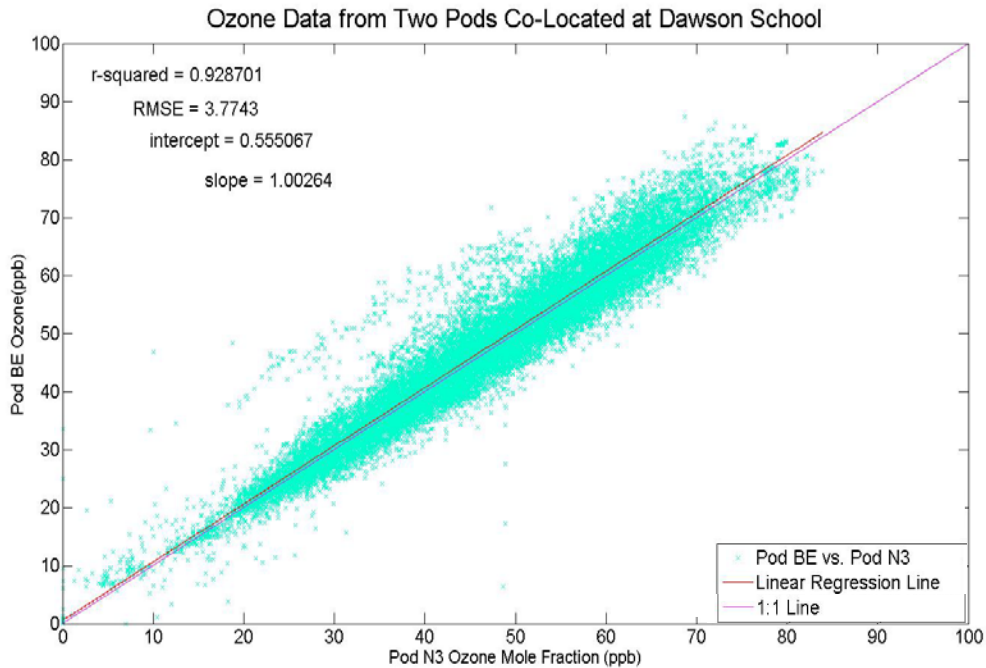


Figure 28: Ozone data from two co-located Pods at the Dawson School Site.

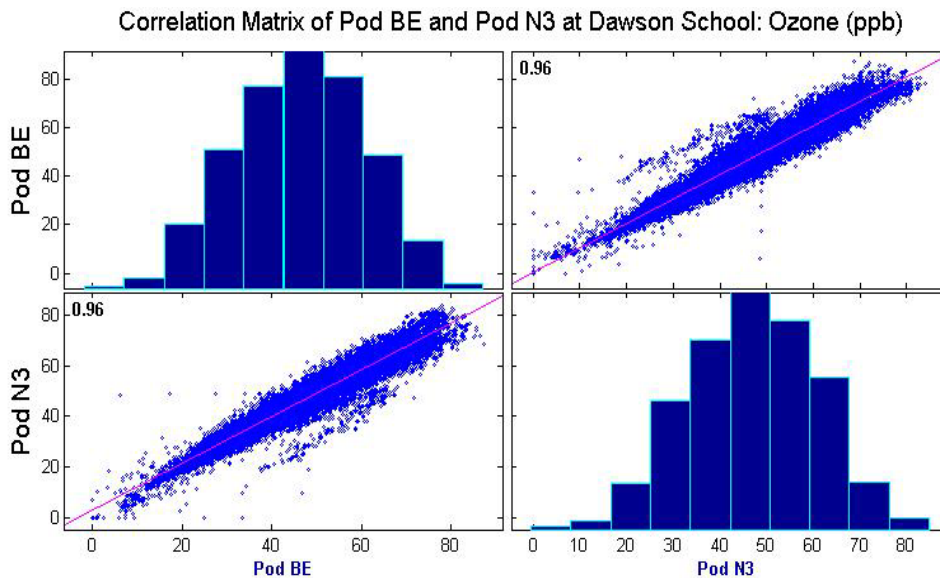


Figure 29: Correlation between Pod BE and Pod N3 Ozone at Dawson School. Histograms for each Pod are shown, in addition the correlation coefficient (r), in the upper left corner of the two scatter plots.

Ozone Correlation among Measurement Sites

The figure below shows a correlation matrix for ozone measured at three of the Boulder County air quality monitoring sites. Data for Boulder County Public Health and Stephen Day Park are excluded due to data quality concerns, as discussed below. Each of the plots shows ozone from a study site (indicated to the left of the row) plotted against ozone from another study site (indicated at the bottom of the column). The correlation

coefficient, r , is given in the top left corner of each graph. The higher this value, the more correlated the ozone at the two sites. In order to see how closely two OG-Pod ozone measurements *could* be to one another, we found the correlation for the ozone measurements from two pods that were co-located right next to each other at Dawson School. Figure 29 shows the correlation coefficient for these two ozone measurements to be 0.96. This is as high a correlation as we could hope to see when comparing two OG-Pod ozone measurements to each other. If the correlation coefficient between two pods at different sites were equal to 0.96, we would take that to mean that there was no significant spatial variability between the two sites. As indicated in Figure 30, correlations of ozone measurements across the study sites range from 0.81 to 0.91, indicating some spatial variability.

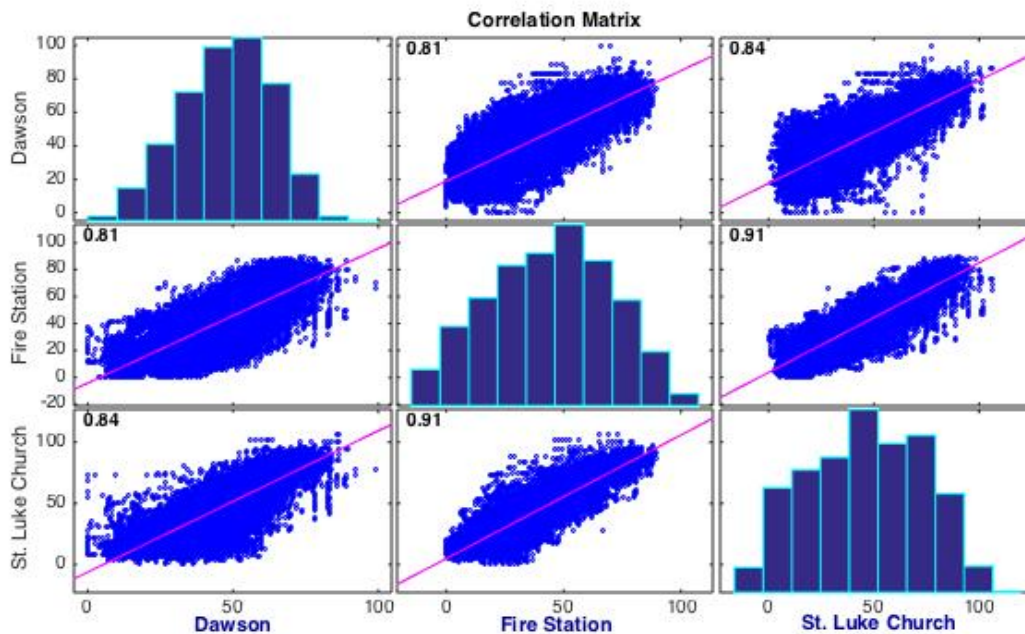


Figure 30: Correlation matrix showing how similar ozone mole fraction (ppb) measurements are at three Boulder County air quality measurement sites. The r -value corresponding to each plot is shown in the top left of each section of the matrix.

Dawson School	1	0.81	0.84
Fire Station	0.81	1	0.91
St. Luke Church	0.84	0.91	1
	Dawson School	Fire Station	St. Luke Church

Table 8: Since the r -values are difficult to read in the figure above, they are presented here in tabular format as well.

The time series of hourly averaged ozone at three study sites is shown below. This plot shows ozone data for the whole summer and weekly plots are included in the appendix. Daytime trends across all of the sites generally track well, as expected for ozone since it is a secondary air pollutant.

Considering all five study sites, some of the trends in ozone were questionable. For example, in some cases the Pod data show spikes of ozone at night. Since ozone formation doesn't occur during the night, this trend seems strange. In cases like this, the environmental parameter space of the model should be checked closely with respect to the environmental parameter space at the study site (namely the ranges encompassed by temperature and relative humidity). There could be reason to discount the

validity of such a trend. The pod located at Boulder County Public Health, in particular, showed trends of increasing ozone at night. The data from this pod is omitted from this report for that reason. Precipitation events often correspond to the pods increasing ozone trends observed at night; thus the connection between these trends and high humidity is being explored further. The pod located at Stephen Day Park had a faulty humidity sensor, and since the calibration equation used is a function of humidity, ozone data from that location has been omitted from the report.

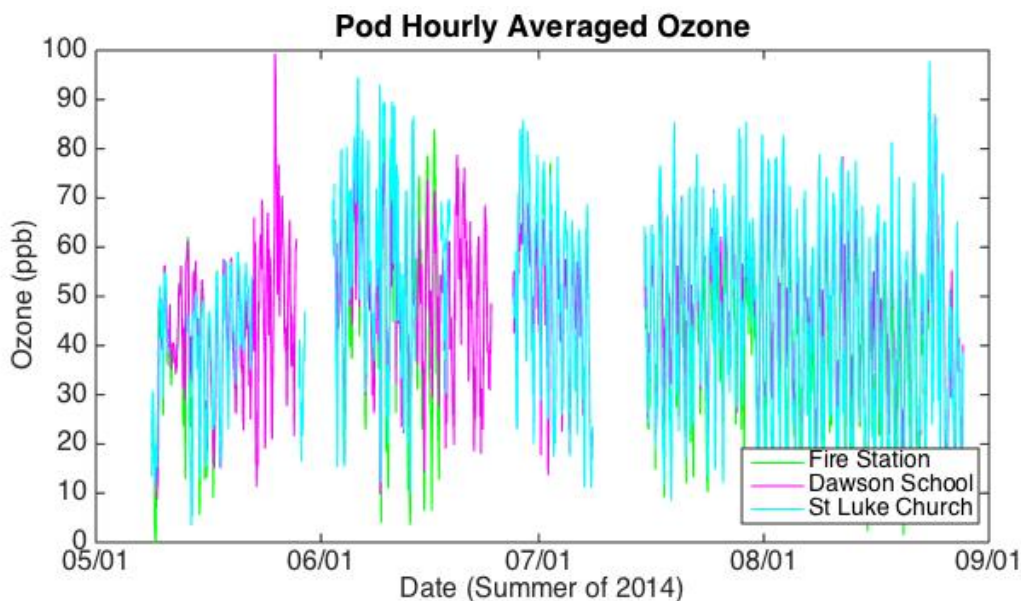


Figure 31: Ozone mole fractions measured at three of the Boulder County measurement sites during the summer of 2014. Weekly plots are shown in the appendix.

Methane

As shown in the Appendix, the calibration functions for methane look promising. We gained access to a methane reference instrument in November. The plots in the Appendix show linear models generated from co-location with a Picarro cavity ring-down methane analyzer. The Picarro and the Pods were housed in a mobile lab. The data shown were collected on two drives through Weld County in the Denver Julesburg Basin, east of Boulder.

The quality of the linear model fits is similar to that of ozone, which is quite good. The weakness of these models in this application, however, lies in the short time frame of the co-location with the Picarro reference instrument, and the environmental parameter space the model was generated in.

Below the calibration function plots for methane, there are histograms that show the parameter space for temperature and humidity from the calibration data as compared to that of the summer measurements at the five air monitoring sites.

During the co-location in the mobile lab with the Picarro instrument, the five pods were all housed together in a small enclosure, and connected to the same air supply as the Picarro. This air was dried before it entered the Picarro, so the humidity during this calibration was virtually zero, and much lower than the humidity at each study site during summer. The small size of the enclosure, and its fairly low air exchange rate yielded fairly high temperatures inside the enclosure, somewhat surprisingly in November. The temperature range during the calibration did not come close to spanning the

temperatures the summer measurements spanned, but rather hugged the upper end of the study site distributions. Due to the poor agreement among these environmental parameter spaces, we will not apply these calibrations to the summer methane sensor signal data.

Discussion

The OG-Pods, used as we have during this study, show promise to offer a low-cost and easily-operable alternative to the status quo in terms ozone monitoring. This tool shows potential to inform interesting trends among ozone and other gases. Comparisons of OG-Pod ozone measurements with those from the Thermo Environmental Instruments Model 49 Ozone Analyzer, co-located Pods at the Dawson School site, and correlations in Pod-measured ozone at three sites across Boulder County indicate good potential for making reliable measurements with these low-cost ozone sensors. However, the quality of the OG-Pod's ozone data (and other gas data) is contingent on how well the mole fraction and environmental parameter space matches among calibration and field deployment. Questionable data showing elevated ozone at night suggest there may also be a need to develop a filter to exclude results for some environmental conditions, such as precipitation events or high relative humidity.

Guidelines for use of the OG-Pods include the following steps:

- Determine the acceptable level of data quality for the application.
- Try to calibrate somewhere with a wider parameter space than will be encountered in your application.
- Measurements may only maintain validity while within model parameter space for all of the following: gas mole fraction, temperature, and humidity.

If monitoring for violations of the NAAQS is the goal, users should ideally utilize a calibration co-location site that experiences higher ozone than was seen at CAMP in Denver during summer 2014. Results found in this study for NO, NO₂ and CO had low signal to noise ratios, indicating the need for further development of the low-cost sensor techniques to measure ambient concentrations of these gases. In addition to ozone, our results show promise for using the Pods to measure CO₂ and methane at ambient levels, provided that appropriate calibration data sets are available.

Moving forward, we are working to better understand Pod data quality, both in terms of optimizing calibration models and in terms of applying those models to quantify sensor signal data. We are hoping to improve our general calibration approach to ensure the full range of variations in the measured species and environmental parameters are covered during calibrations. Additionally, we plan to examine individual terms in calibration models to see how much weight each term carries. The terms in calibration models include sensor response, relative humidity, and temperature. Quantifying the relative weight of each term in the model will help us to better understand overall measurement responses and when data might need to be excluded because a contributing measurement is outside the range encompassed in the calibration.

Appendix

Sensor Operating Principles

Metal Oxide:

Principle: Oxidation and reduction reactions on a thin metal film change the electrical resistance across the thin film on the surface of the sensor.

- Thin film such as SnO_2 is heated
- O_2 adsorbs to the surface
- Fewer electrons can flow
- Reducing gas (like CH_4) removes some O_2 from the surface
- More electrons can flow (current increases)

Sensors operating on this principle: O_3 , CH_4 , Total VOCs, NO_2 , and CO

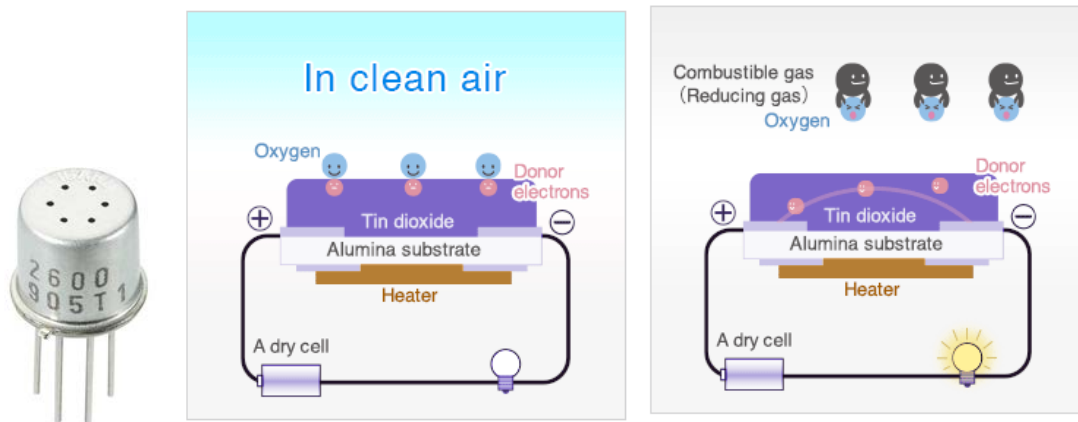


Figure A1: A metal oxide type sensor is pictured here, next to cartoons of its operational principle.

Source of Images: <http://www.figaro.co.jp/en/technicalinfo/principle/mos-type.html>

Electrochemical:

Principle: Similar to a battery, a potential difference is imposed across two electrodes that are separated by an electrolytic solution.

- Gases pass through porous membrane
- Membrane properties can be used to adjust response
- In the presence of clean air \rightarrow The counter and working electrodes at same potential
- Oxidizing gas at working electrode \rightarrow The counter electrode potential changes due to charge transfer
- Current can be inferred by measuring V_{ref} \rightarrow gas concentration
- Potentiostat keeps the working electrode at a constant potential

Sensors operating on this principle: NO

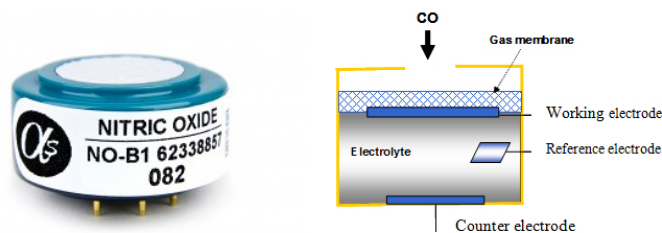


Figure A2: An electrochemical type sensor is pictured here, next to a cartoon of its operational principle.

Picture source: <http://www.ti.com/ww/en/industrial/sensors/Gas/learn.html>

Non-Dispersive Infrared

Principle: Light Absorption

- CO₂ absorbs infrared light at a specific frequency.
- A lamp at this frequency illuminates a very small optical cavity
- The more CO₂ in the optical cavity, the more light is absorbed, and the less light is incident on the detector.

Sensors operating on this principle: CO₂

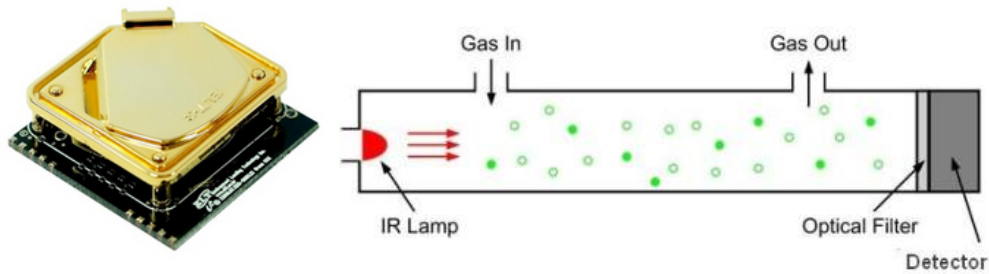


Figure A3: A non-dispersive infrared type sensor is pictured here, next to a cartoon of its operational principle.

Picture Source: <http://www.co2meter.com/blogs/news/6010192-how-does-an-ndir-co2-sensor-work>

Methane Calibration Functions:

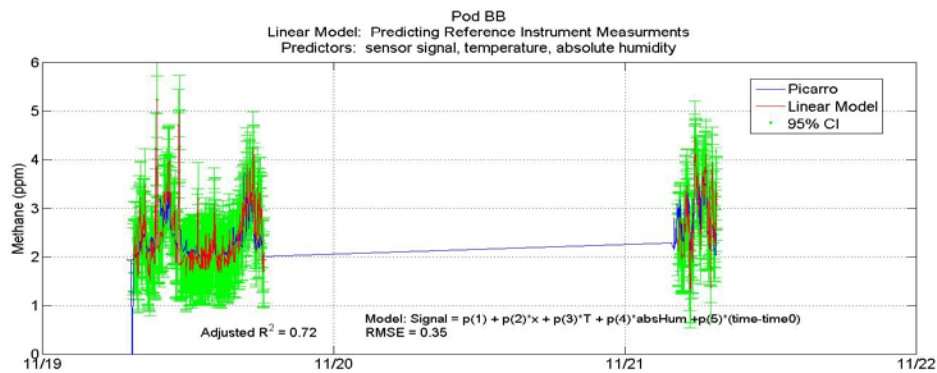


Figure A4: Calibration function for Pod BB methane.

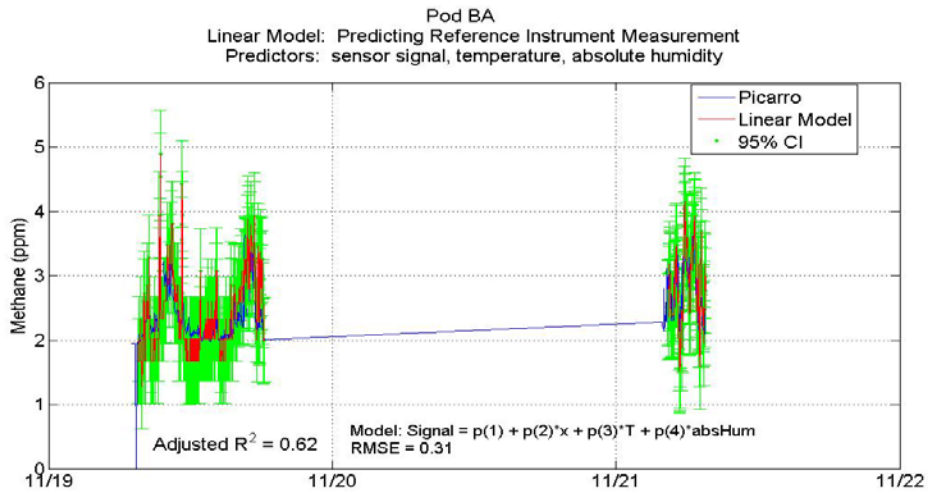


Figure A5: Calibration function for Pod BA methane.

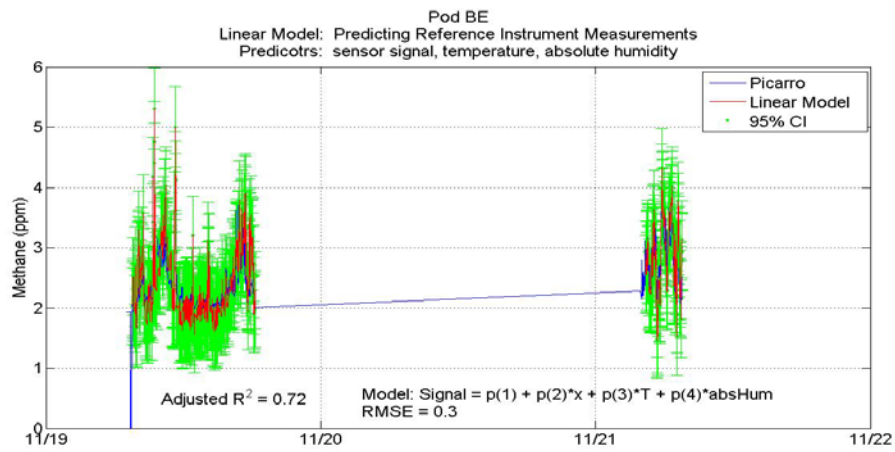


Figure A6: Calibration function for Pod BE methane.

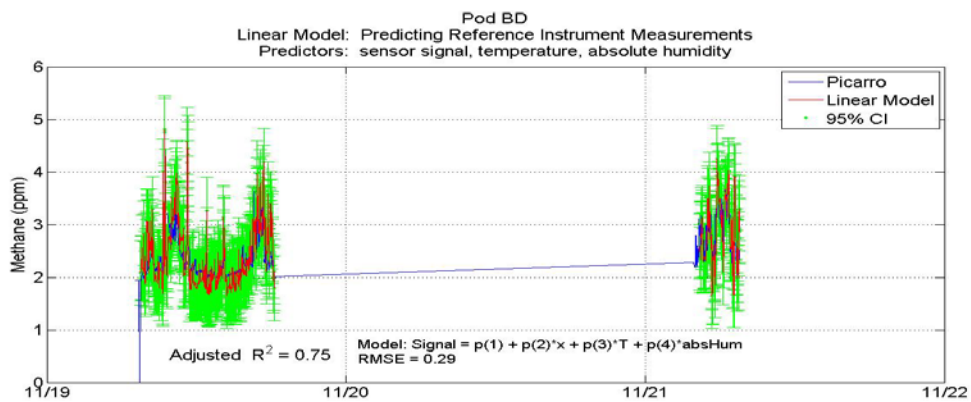


Figure A7: Calibration function for Pod BD methane.

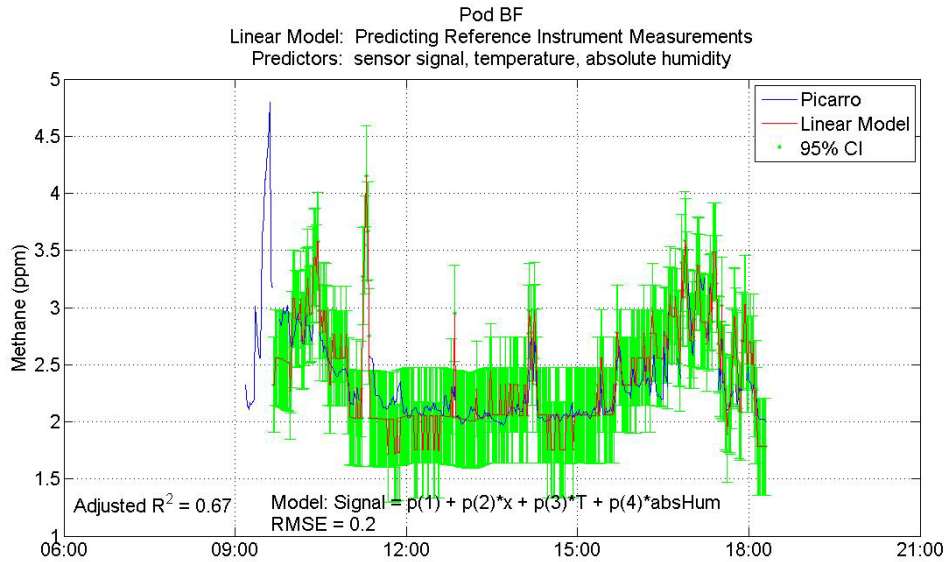


Figure A8: Calibration function for Pod BF methane.

Parameter space comparison for methane co-location and BC data for temperature and Humidity:

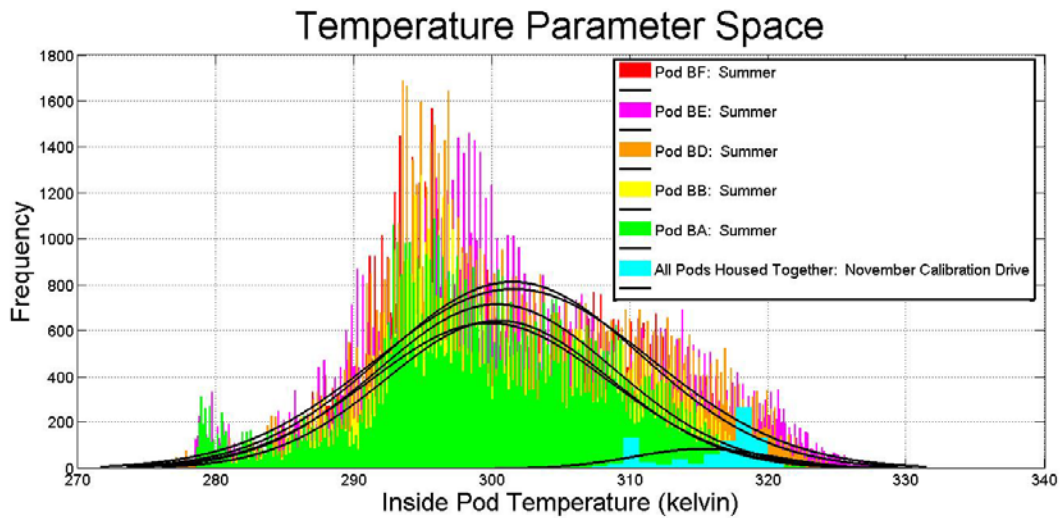


Figure A9: This plot shows overlaid histograms of the parameter space for temperature from the five measurement sites, with the temperature parameter space from the methane calibration in blue, in front of them all, hugging only the high end of the temperatures from the measurement sites.

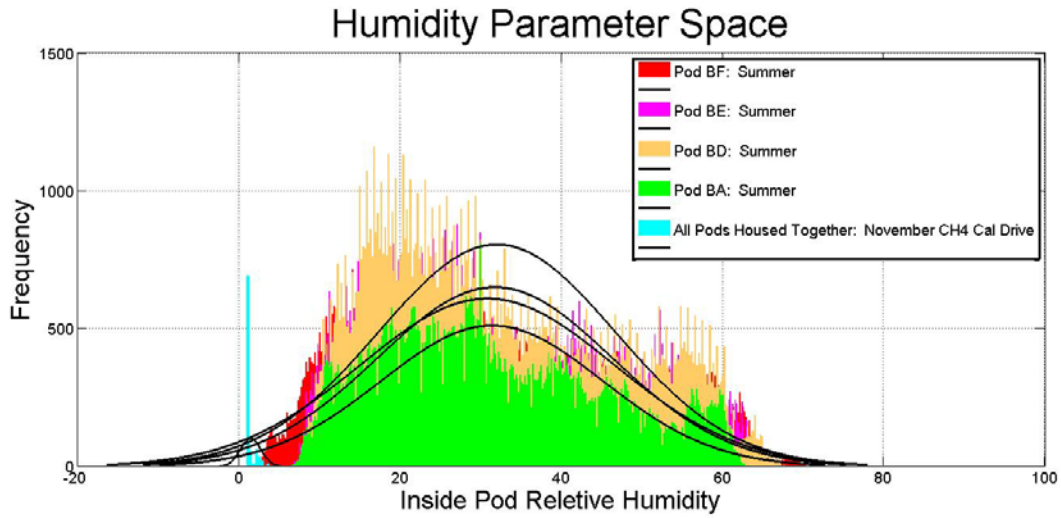


Figure A10: This plot shows overlaid histograms of the parameter space for humidity from the five measurement sites, with the humidity parameter space from the methane calibration in blue, in front of them all, and below almost all of the humidity at the study sites over the summer.

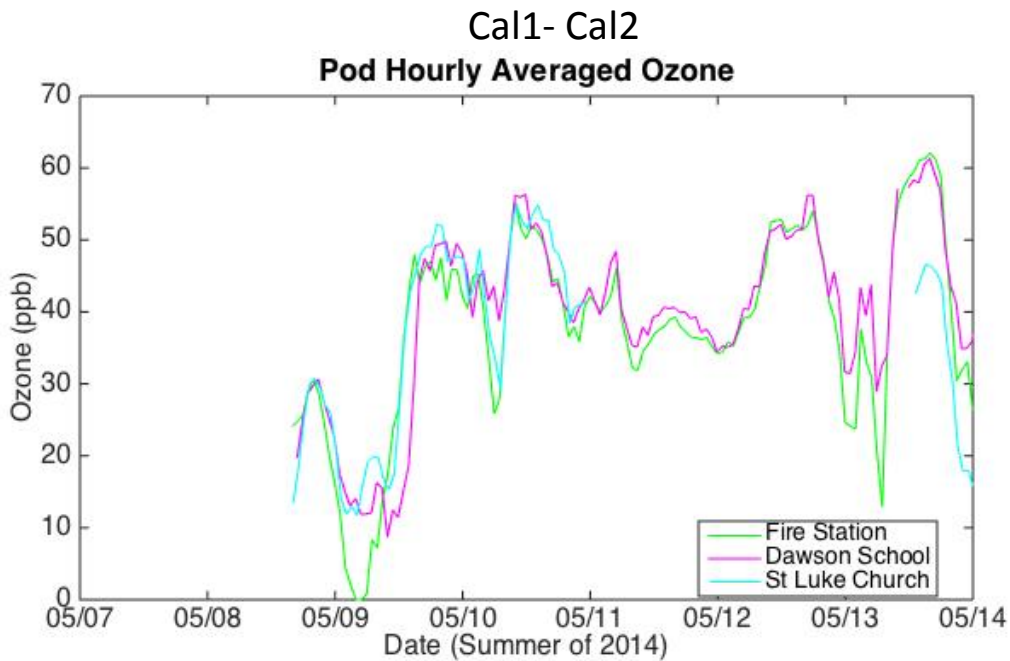


Figure A11: Hourly averaged ozone at three Boulder County measurement sites from May 7th to May 14th.

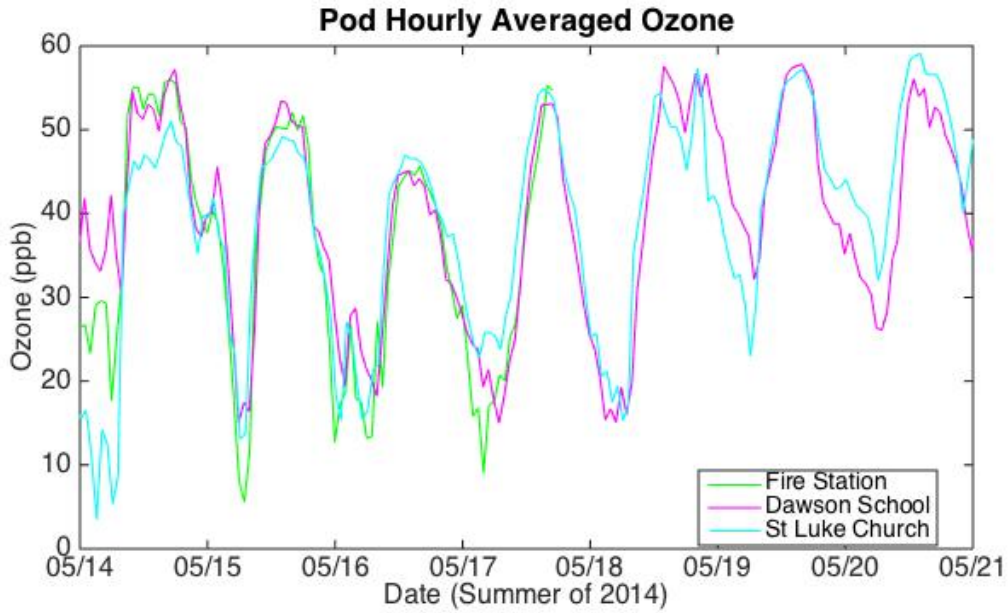


Figure A12: Hourly averaged ozone at three Boulder County measurement sites from May 14th to May 21st.

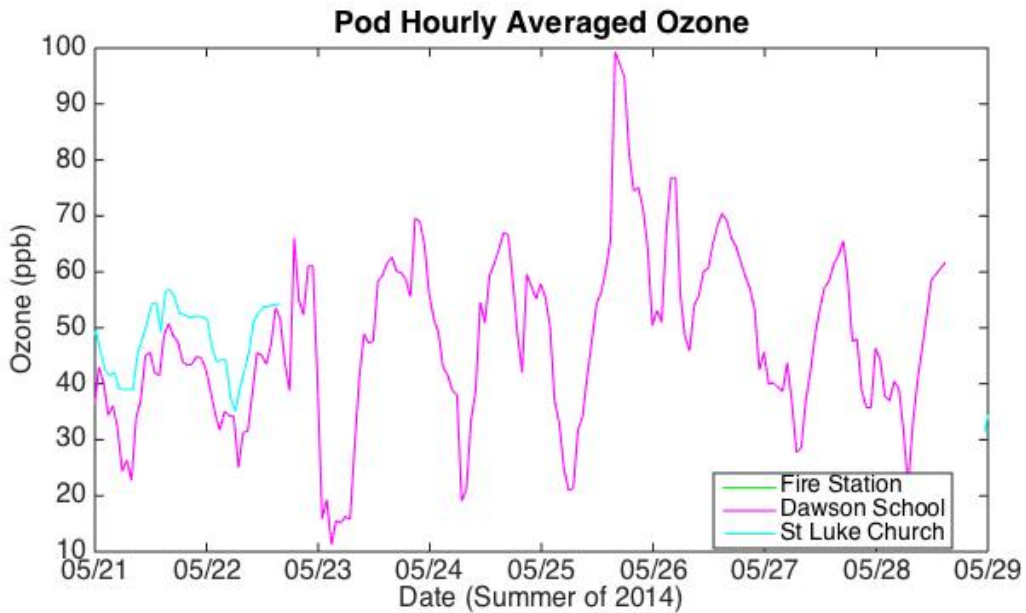


Figure A13: Hourly averaged ozone at three Boulder County measurement sites from May 21st to May 29^h.

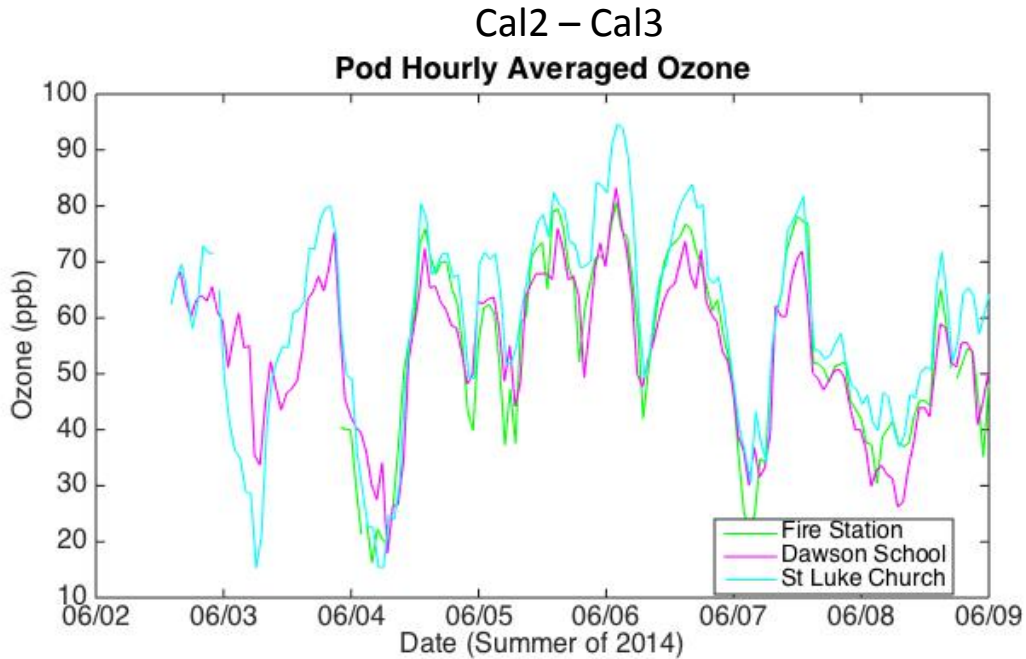


Figure A14: Hourly averaged ozone at three Boulder County measurement sites from June 2nd to June 9th.

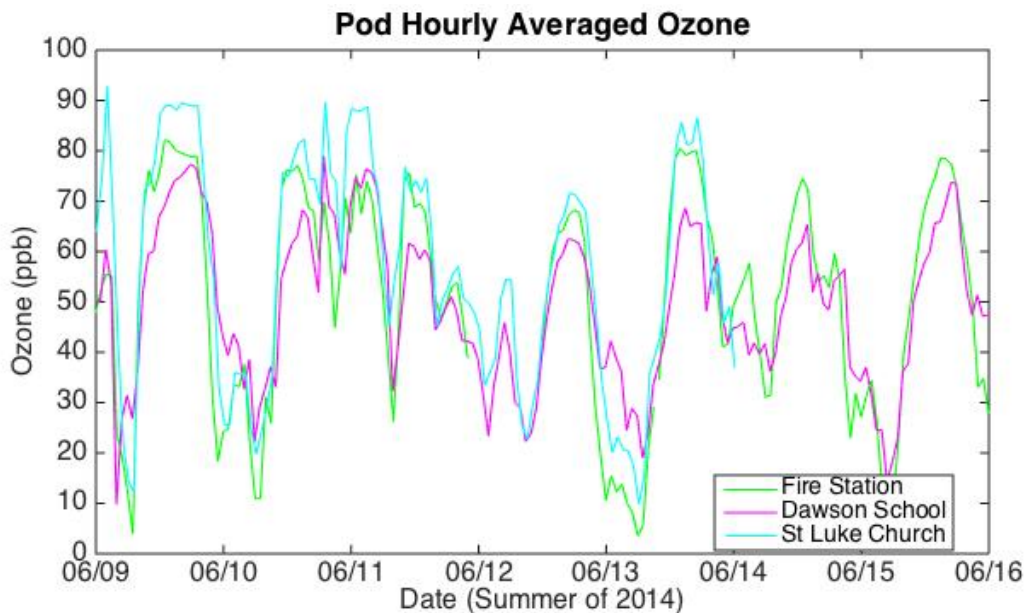


Figure A15: Hourly averaged ozone at three Boulder County measurement sites from June 9th to June 16th.

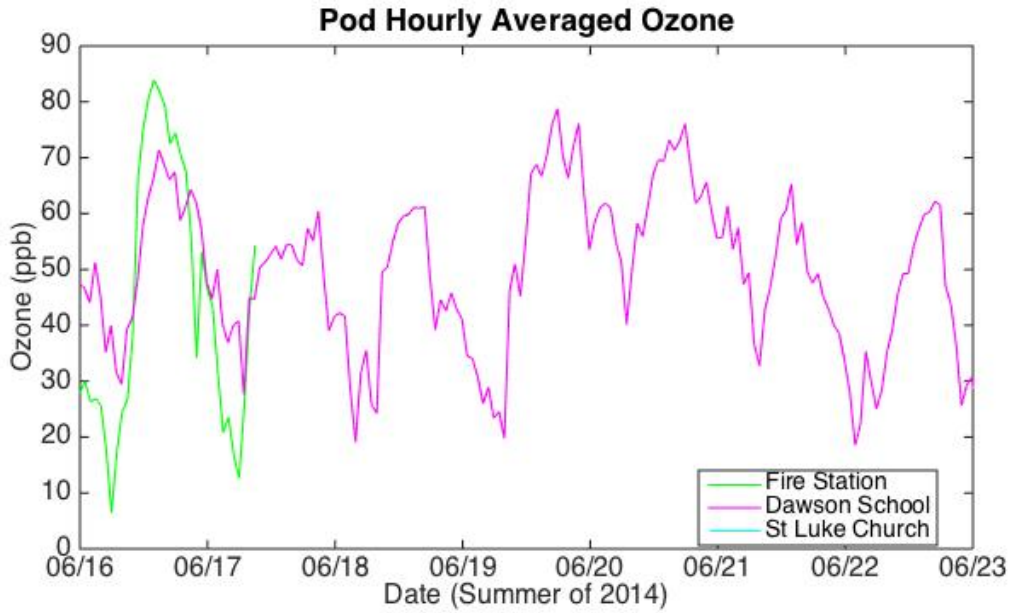


Figure A16: Hourly averaged ozone at three Boulder County measurement sites June 16th to June 23rd.

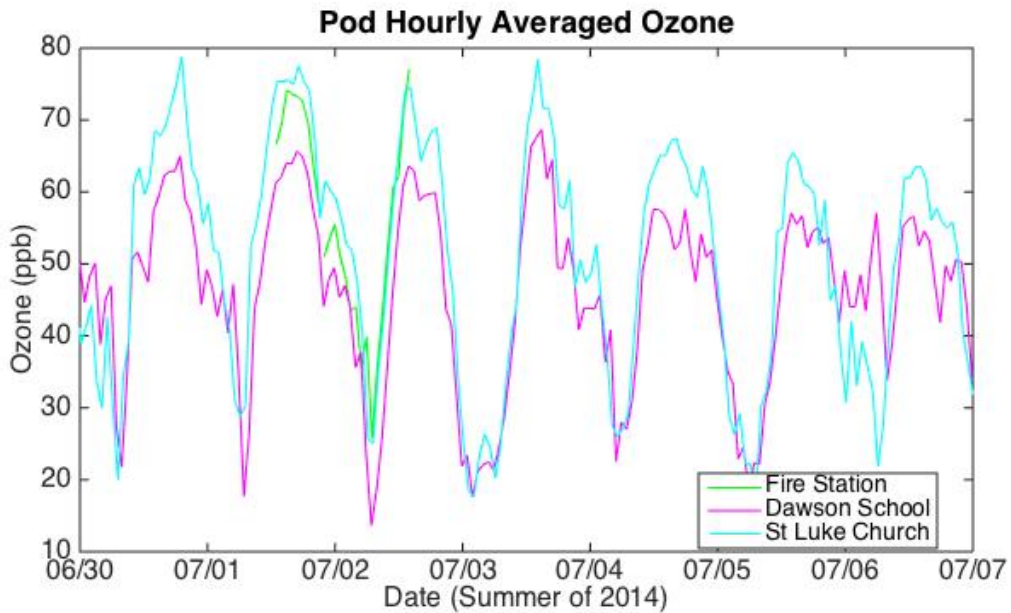


Figure A17: Hourly averaged ozone at three Boulder County measurement sites from June 30th to July 7th.

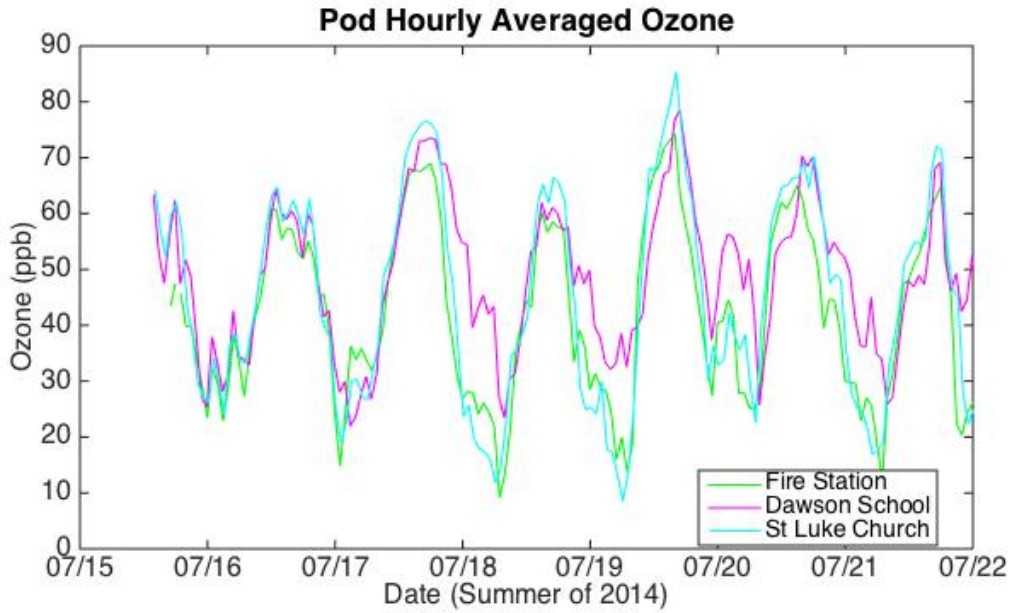


Figure A18: Hourly averaged ozone at three Boulder County measurement sites from July 15th to July 22nd.

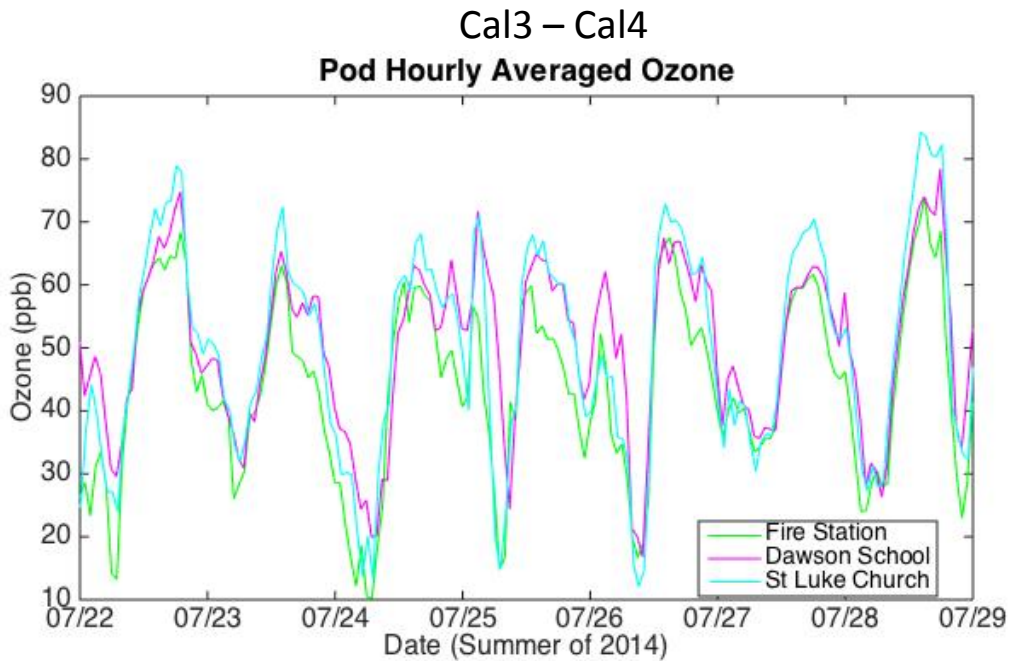


Figure A19: Hourly averaged ozone at three Boulder County measurement sites from July 22nd to July 29th.

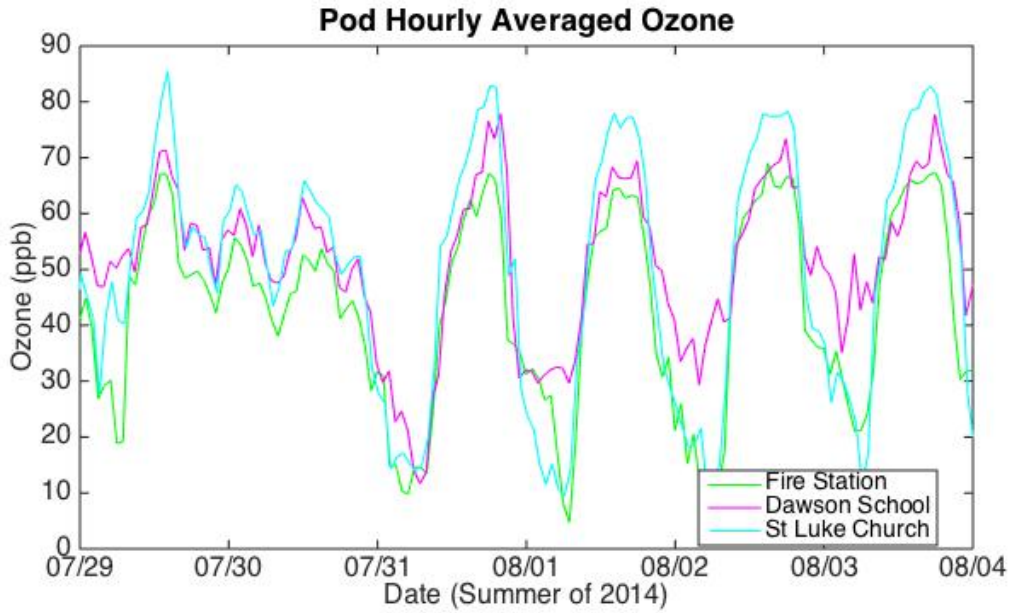


Figure A20: Hourly averaged ozone at three Boulder County measurement sites from July 29th to August 4th.

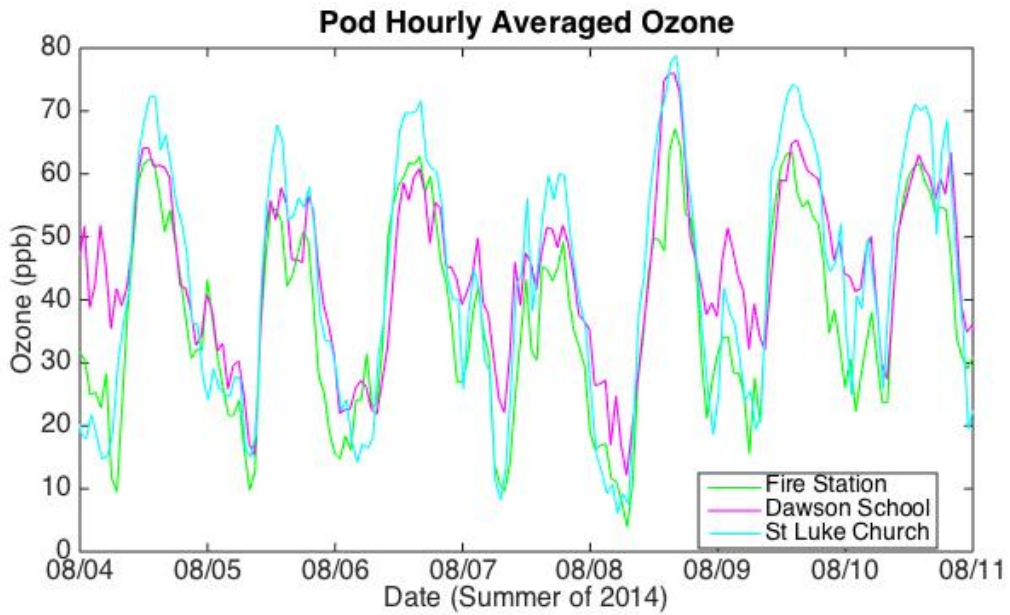


Figure A21: Hourly averaged ozone at three Boulder County measurement sites from August 4th to August 11th.

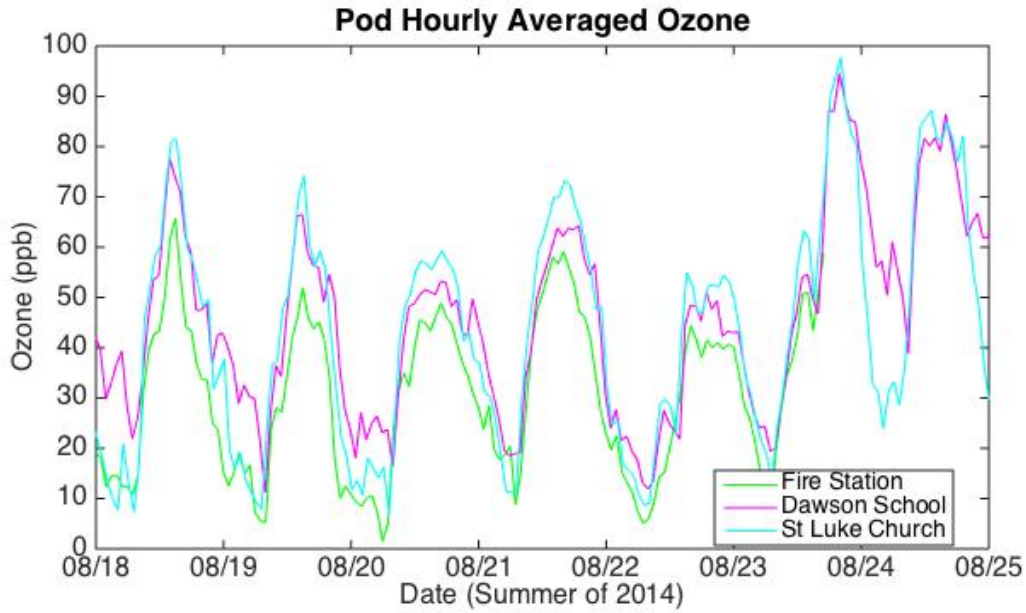


Figure A22: Hourly averaged ozone at three Boulder County measurement sites from August 18th to August 25th.

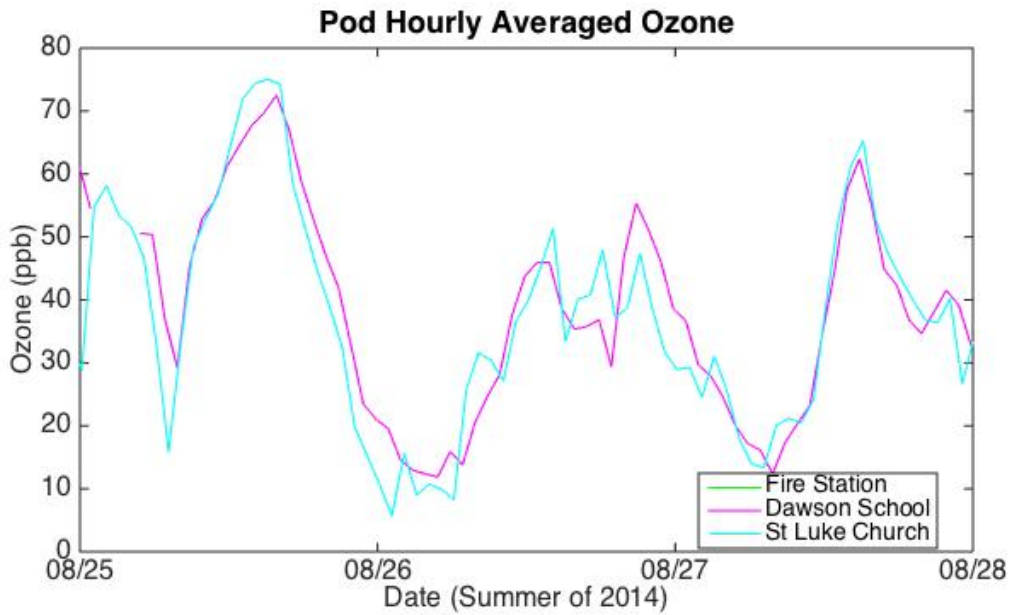


Figure A23: Hourly averaged ozone at three Boulder County measurement sites from August 25th to August 28th.